



Influence of the Keystone Grazer, *Sesarma reticulatum*, on the Hydrology and Organic Matter Cycling in Salt Marshes of the Southeastern USA

Elise S. Morrison¹ · Thomas S. Bianchi² · William F. Kenney³ · Mark Brenner^{2,3} · Kimberly Prince^{1,4} ·
Sydney Williams¹ · Collin Ortals¹ · Orlando Cordero¹ · Sinéad M. Crotty^{1,5} · Christine Angelini¹

Received: 6 April 2023 / Revised: 16 January 2024 / Accepted: 13 February 2024 / Published online: 9 March 2024
© The Author(s) 2024

Abstract

In salt marshes of the Southeastern USA, purple marsh crabs (*Sesarma reticulatum*), hereafter *Sesarma*, aggregate in grazing and burrowing fronts at the heads of tidal creeks, accelerating creek incision into marsh platforms. We explored the effects of this keystone grazer and sediment engineer on salt marsh sediment accumulation, hydrology, and carbon (C) and nitrogen (N) turnover using radionuclides (^{210}Pb and ^{7}Be), total hydrolyzable amino acids (THAA), and C and N stable isotopes ($\delta^{13}\text{C}$ and $\delta^{15}\text{N}$) in sediment from paired *Sesarma*-grazed and un-grazed creeks. *Sesarma*-grazed-creek sediments exhibited greater bioturbation and tidal inundation compared to sediments in un-grazed creeks, as indicated by larger ^{210}Pb and ^{7}Be inventories. Total organic carbon (TOC) to total nitrogen (TN) weight ratios (C:N) were higher and $\delta^{15}\text{N}$ values were lower in grazed-creek sediments than in un-grazed-creek sediments, suggesting *Sesarma* remove and assimilate N in their tissues, and excrete N with lower $\delta^{15}\text{N}$ values into sediments. In support of this inference, the percent total carbon (TC) and percent TOC declined by nearly half, percent TN decreased by ~80%, and the C:N ratio exhibited a ~threefold increase between *Sesarma* fore-gut and hind-gut contents. An estimated 91% of *Sesarma*'s diet was derived from *Spartina alterniflora*, the region's dominant salt marsh plant. We found that, as *Sesarma* grazing fronts progress across marsh landscapes, they enhance the decay of *Spartina*-derived organic matter and prolong marsh tidal inundation. These findings highlight the need to better account for the effects of keystone grazers and sediment engineers, like *Sesarma*, in estimates of the stability and size of blue C stores in coastal wetlands.

Keywords Blue carbon · Sesarmid crabs · Salt marsh · Biomarker · Radionuclide · Herbivory · Coastal wetland

Introduction

Coastal ecosystems, such as salt marshes, mangrove forests, and seagrass meadows, are recognized as blue carbon (C) habitats because of their capacity to capture and store

Communicated by Angelos Hannides

Key Points

- *Sesarma*-grazed creeks exhibit greater bioturbation and more prolonged tidal inundation, indicated by larger radionuclide (^{210}Pb and ^{7}Be) inventories.
- The *Sesarma* diet is composed predominantly of *Spartina alterniflora*, highlighting its role as a keystone grazer in salt marshes.
- *Sesarma* significantly alter the carbon and nitrogen content of salt marsh organic matter.

Extended author information available on the last page of the article

C (Macreadie et al. 2019; Temmink et al. 2022). They are also habitats for many species of commercial interest and facilitate the exchange of organic matter (OM) between terrestrial and marine systems (Macreadie et al. 2019; Vaughn et al. 2020; McLeod et al. 2011; Hinson et al. 2017; Duarte et al. 2008; Windham-Myers et al. 2018). These critical habitats are vulnerable to many threats, including sea-level rise and land-use change (Macreadie et al. 2019; Bianchi and Morrison 2018; Langston et al. 2021; Ganju et al. 2017), and are being lost at a rate of 1–7% yr^{-1} globally (Duarte et al. 2008; Hopkinson et al. 2012). The ecosystem services provided by blue C habitats can be altered by many factors, including interactions between plants, animals, and sediments. Feedbacks between biology and morphodynamics can also influence the structure and function of tidal systems, subsequently affecting the exchange of water, OM, sediment, and nutrients (Kearney and Fagherazzi 2016). Evaluating

these plant-animal-sediment interactions is essential not only to quantify the ecosystem services of blue C habitats (Costanza et al. 2017), but also to accurately represent them in Earth System models (Ward et al. 2020) and evaluate their role in global nutrient cycles (Macreadie et al. 2019; Xiao et al. 2021).

Benthic macroinvertebrates alter the physical and chemical properties of sediments through bioturbation, bioirrigation, and grazing, thereby influencing OM turnover and associated C and nitrogen (N) cycling (Laverock et al. 1627; Snelgrove et al. 2018; Middelburg 2018; He et al. 1814; Bianchi et al. 2021). Bioturbation, the physical disruption of sediment via burrowing, can extend the oxic zone deeper into sediments and promote particle reworking (Aller 1980). Faunal activity can also promote bioirrigation, whereby water is transported in and out of the sediment through burrows, allowing for enhanced solute exchange and increased oxygen flux between burrows and the overlying water column (Aller 1980; Aller and Cochran 2019; Michaud et al. 2009; Perger et al. 2023). These physical and chemical alterations affect redox-sensitive biogeochemical processes and can enhance microbial activity, increase fluxes of O₂ and dissolved inorganic N into sediments, and enhance OM decomposition (Middelburg 2018; Aller and Cochran 2019; Laverock et al. 2011; Kristensen and Kostka 2005; Kristensen 2000). Simultaneously, faunal grazing on marsh plants can influence coastal wetland biogeochemistry (Zhang et al. 2019; Silliman and Bortolus 2003) and significantly reduce belowground C in coastal wetland sediments (He et al. 1814). Faunal activities can also interact with other ecological and climate stressors; for instance, extensive marsh sediment erosion and cordgrass loss have been caused by synergistic interactions between sea-level rise and the purple marsh crab, *Sesarma reticulatum* (hereafter *Sesarma*) (Crotty et al. 2020, 2017; Hughes et al. 2009).

Sesarma has recently been recognized as an emergent keystone grazer and sediment engineer in US Atlantic salt marshes (Crotty et al. 2020; Hughes et al. 2009; Holdredge et al. 2009; Wilson et al. 2012; Farron et al. 2020). Although native to the east coast of North America (Abele 1973), its distribution and abundance have been altered by overfishing of estuarine fish and blue crabs (*Callinectes sapidus*) in the Northeastern USA (Altieri et al. 2012; Bertness et al. 2009) and sea-level rise in the Southeastern USA (Crotty et al. 2020). In the Southeastern USA, where this study is focused, *Sesarma* have caused die-offs of *Spartina alterniflora* (Bertness et al. 2014) and created grazed and intensively burrowed “fans” along tidal creek heads, which have increased in coverage by 10–29% in < 25 years (Crotty et al. 2020).

These grazing and burrowing activities of *Sesarma* have resulted in de-vegetated creek heads that accelerate creek elongation rates by 2–5 m per year (versus 0.5–1 m per year for un-grazed creeks) (Wu et al. 2021), reduce invertebrate biomass (Crotty et al. 2020), increase below-ground biomass decomposition (Wilson et al. 2012), and lead to enhanced erosion potential (Wilson et al. 2012; Vu and Pennings 2021) and greater hydraulic exchange capacity (Crotty et al. 2020).

Although the geomorphic and ecological consequences of plant-animal-interactions have been explored (Crotty et al. 2020), additional investigations into *Sesarma*’s effects on marsh biogeochemistry are needed (He et al. 2020), as this species’ burrowing and grazing activities differ substantially from others that have been previously investigated. For instance, mud fiddler crabs (*Uca pugnax*) excavate shallow burrows and do not consume live macrophytes, whereas *Sesarma* excavate deep, extensive burrows and actively graze on macrophyte leaves and roots (Smith and Tyrrell 2012). Additionally, further study of the effect of sesarmid crabs (Family Sesarmidae) on salt marsh biogeochemistry is needed. Sesarmids can influence litter turnover and decomposition in mangroves (Kristensen 2008) and marshes (Altieri et al. 2012; Holdredge et al. 2009), and in mangroves, they are key regulators of OM export, nutrient cycling, and decomposition (Friesen et al. 2018), capable of removing 30–90% of annual litter production (Robertson 1986; Micheli 1993; Slim et al. 1997). However, Sesarmids’ effects on salt marsh biogeochemistry are understudied relative to their effects on mangrove ecosystems.

While *Sesarma* grazing on marsh creek heads has been studied, less is known about this keystone grazer’s effects on sedimentation, hydrology, and OM cycling (including components C and N). Given the scale and rate at which *Sesarma* are modifying the geomorphology of Southeastern US salt marshes, and the potential negative effects of crab activity on C storage (Guimond et al. 2020), further investigation into their role in salt marsh sedimentation, hydrology (via radionuclides), and OM cycling (via amino acids and stable isotopes) is warranted. We therefore analyzed radionuclides and biomarkers in sediments of *Sesarma*-grazed and un-grazed creeks in Georgia salt marshes to evaluate crab-driven effects on marsh sediment inundation, OM composition, and C and N cycling, and to address the following hypotheses:

- 1 Radionuclide (²¹⁰Pb and ⁷Be) inventories (dpm cm⁻²) and maximum depths of detection are greater in *Sesarma*-grazed creeks, when compared to un-grazed creeks, indicating greater input of ²¹⁰Pb and ⁷Be to sediments and greater bioturbation in grazed creeks.

- 2 *Sesarma*-grazed creeks have greater drainage ratios (i.e., relative to the creek's length and associated tidal prism, grazed creeks drain relatively larger areas of adjacent marsh than their un-grazed counterparts), and greater ^{7}Be inventories (i.e., fluxes) indicate that grazed marsh platforms are inundated longer than un-grazed creeks.
- 3 *Sesarma* absorb N in their gut, and because of isotope fractionation between trophic levels, are themselves enriched in ^{15}N and excrete N with lower $\delta^{15}\text{N}$ values. This is reflected by declines in N content, $\delta^{15}\text{N}$ values, and total hydrolysable amino acids (THAA) in OM from the fore- to hind-gut.
- 4 Grazed creeks retain the isotope values caused by *Sesarma* OM processing, as seen by lower $\delta^{15}\text{N}$ values in grazed-creek sediments.

Methods

Site Description

Samples were collected from four pairs of grazed and un-grazed creeks (Creek Pairs A–D) distributed across approximately 134 km² of salt marsh on Sapelo Island and Little Sapelo Island, Georgia (Fig. 1). This region experiences semi-diurnal tides that range from 1.5 to 2.8 m over neap to spring tide cycles. NOAA's tidal estimates for the nearest station (Old Tea Kettle Creek, GA; Station 8675365) in June 2018 showed that the tidal maximum and minimum were 2.55 m and –0.29 m, respectively, whereas the maximum tide for October 2017 (9 months

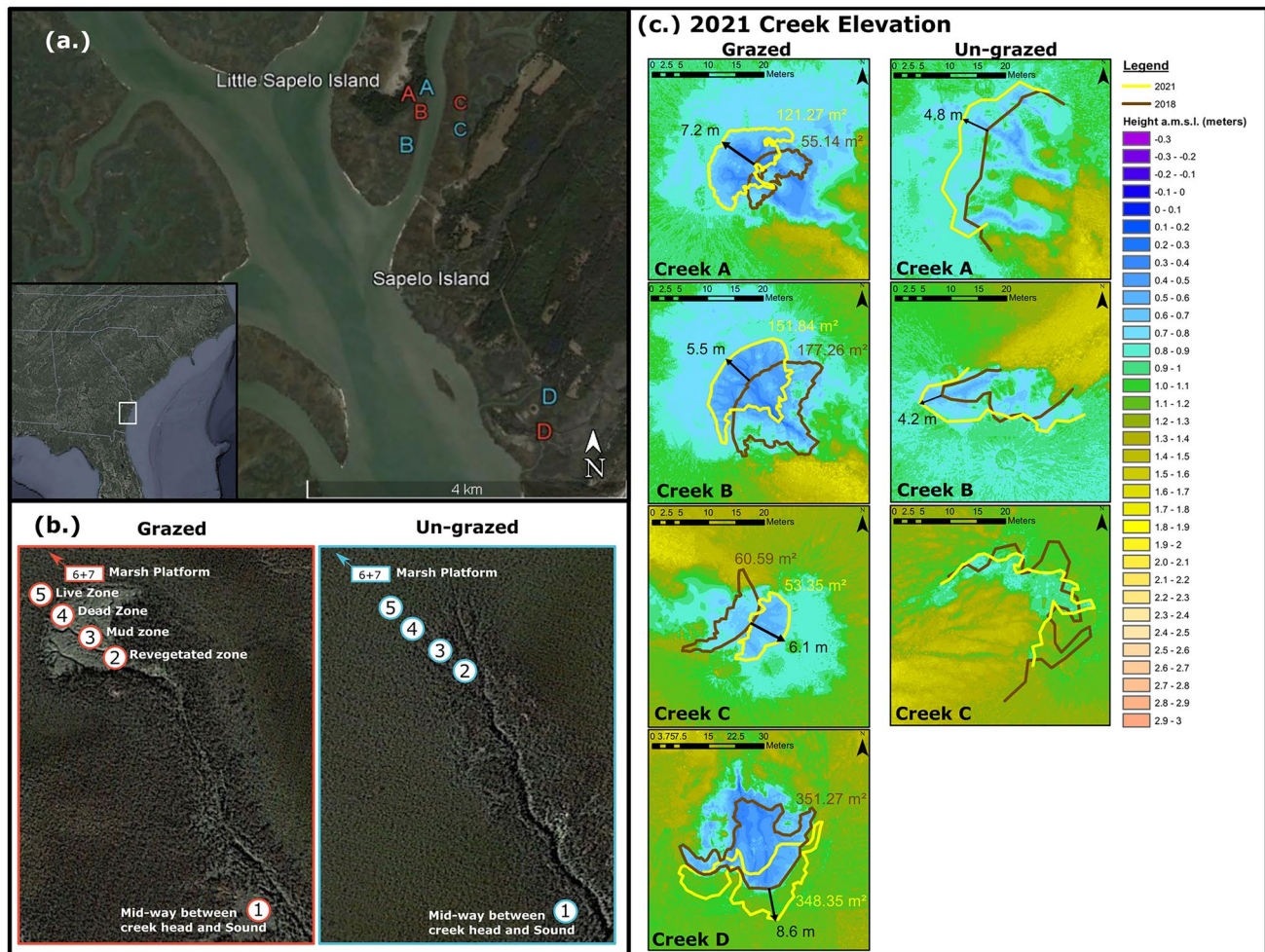


Fig. 1 **a** Paired creek locations on Little Sapelo and Sapelo Island, GA. red, grazed; blue, un-grazed. **b** Paired grazed and un-grazed creeks A, with marked zone designations. **c** Digital elevation model of all creek pairs in 2021, except for the un-grazed Creek D. For grazed creeks, the area of each bare mudflat is shown for 2018 (red; concurrent with sediment sample collection) and 2021 (yellow). The

direction and distance of creek incision is noted with black arrows/text at the head of each creek. Since un-grazed creeks did not have bare mudflats, the transition from runnels to marsh flat is noted for 2018 (red) and 2021 (yellow). Due to creek meandering and dense vegetation, we were unable to capture more than a few meters of creek incision with terrestrial lidar

prior to sample collection) was 2.51 m, and the minimum tide was -0.07 m. Sampled creeks were selected based on similarities in creek length, proximity to Doboy Sound, and hydrology. Creek pairs were initially selected using aerial photos, and grazing status was confirmed with a field survey in 2018, prior to sample collection. Grazed creeks were defined as those in which *Sesarma* grazing began > 10 years prior to sampling, following the definition of grazed creeks in Crotty et al. (2020). Whereas drivers of salt marsh invertebrate distributions can occur on timescales both greater or less than 10 years (Rochlin and Morris 2017), the 10-year cutoff was selected to be consistent with the study of Crotty et al. (2020). Un-grazed creeks were those with no *Sesarma* present, had no indication of *Sesarma* grazing or burrowing, and were within 250 m of their paired grazed creek. Whereas un-grazed creeks may have experienced some grazing and bioturbation from invertebrate species other than *Sesarma*, they did not exhibit the extensive grazing and burrows that are characteristic of *Sesarma* activity, which results in de-vegetated swathes of marsh (Crotty et al. 2020; Vu and Pennings 2021; Vu et al. 2017).

A digital elevation model (DEM) was constructed for each creek, with the exception of un-grazed Creek D, using terrestrial laser scans acquired with a Riegl VZ-400 scanner during sampling trips in 2018 and in 2021. The generated point cloud was processed with lastools (rapidlasso GmbH, Gilching, Germany, version 201003) to mitigate noise, reduce error, and identify ground points (Isenburg 2020). Elevation data were referenced to NAVD 88 and collected with a Trimble Geo 7X GNSS unit, using RTK (Fig. 1).

Seven creek zones were designated based on grazed creek characteristics and past studies (Crotty et al. 2020; Wu et al. 2021; Vu et al. 2017) and were numbered according to distance from Doboy Sound, with Zone 1 closest to the Sound and Zone 7 farthest from the Sound (Fig. 1). Zone 1 was located midway between the Sound and the creek head; Zone 2 was the region of recent grazing that exhibited *Spartina alterniflora* regrowth; Zone 3 was the region of the creek head with soft sediment and no vegetation; Zone 4 was the region with firm sediment and the greatest *Sesarma* burrow density along the creek head; Zone 5 was the region directly adjacent to Zone 4 but had live *Spartina* present. Zones 6 and 7 were the low- and high-marsh platforms, which were 15 m and 30 m from the creek head, respectively. Un-grazed creek zone characteristics were markedly different from those of grazed creeks, but equivalent zones were identified using creek morphology and distance to the Sound and/or creek head (Fig. 1).

Differences in the grazed- and un-grazed-creek invertebrate communities are notable (Crotty et al. 2020). Un-grazed creeks have much greater invertebrate biomass than *Sesarma*-grazed creeks, with communities dominated by ribbed mussels (*Gukensia demissa*) and fiddler crabs (*Uca*

pugnax). The marsh platforms of un-grazed creeks also have much greater benthic invertebrate biomass than those of *Sesarma*-grazed creeks and are dominated by ribbed mussels (*Gukensia demissa*), fiddler crabs (*Uca pugnax*), and snails (*Littoraria irrorata*). In contrast, the creek and marsh platform of *Sesarma*-grazed creeks have invertebrate communities dominated by *Sesarma*, which are 80 times more abundant in *Sesarma*-grazed creeks (Crotty et al. 2020).

Radionuclides

Radionuclides (^{210}Pb and ^7Be) in sediment cores were used to evaluate crab-mediated sediment bioturbation and marsh sediment inundation, as an indicator of local hydrological changes. $^{210}\text{Pb}_{\text{xs}}$ has a half-life of 22.3 years and is typically measurable in core sediments as long as 130 years after deposition (Appleby 2008). The sediment stratigraphy of $^{210}\text{Pb}_{\text{xs}}$ activity reflects the combined effects of ecological and sedimentation processes over intervals of years to decades. Because of its short half-life (53.1 days), ^7Be persists in the environment for only ~ 0.75 years. For this reason, the sediment inventory of ^7Be reflects ecosystem processes (e.g., rainfall, bioturbation) that occurred in the ~ 9 months before core collection. We measured $^{210}\text{Pb}_{\text{xs}}$ to infer marsh conditions over the last several decades and ^7Be data provided insights into very recent (< 1 year) marsh conditions.

Four cores were collected for radionuclide measurements in June 2018, from grazed and un-grazed creeks at Creek Pair B, in Zone 3 (the creek head zone) and Zone 6 (15 m from creek head in the low marsh platform). Four additional cores were collected for radionuclide measurements in October 2021, from grazed and un-grazed creeks at Creek Pair A, in Zone 3 (the creek head zone) and Zone 6 (15 m from the creek head, in the low marsh platform). Cores were collected using a piston corer with a 6.99-cm-ID polycarbonate core barrel. Cores were kept at 4°C after collection and sectioned into 1-cm intervals within 24 h. Samples were then frozen, freeze-dried, and ground to a fine powder with a roller mill. Radiometric measurements (^7Be , ^{210}Pb , and ^{226}Ra) were made using low-background gamma counting with well-type intrinsic germanium detectors (Schelske et al. 1994). The time required to complete ^7Be measurements was dependent on the depth of ^7Be in the sediment cores, with deeper (older) sediments requiring longer count times because of their relatively lower activities. ^7Be measurements were completed within 30 days for the 2018 cores and 75 days for the 2021 cores. Unsupported ^{210}Pb activity ($^{210}\text{Pb}_{\text{xs}}$) in each sample was determined by subtracting ^{226}Ra activity (i.e., supported ^{210}Pb activity) from total ^{210}Pb activity. We calculated sediment ages with the constant-flux, constant-sedimentation (CFCS) model (Krishnaswamy et al. 1971). We estimated the average mass sedimentation rate (MSR, $\text{mg cm}^{-2} \text{a}^{-1}$) and activity at the time of deposition

(A_0) by minimizing the sum of the negative log-likelihood (NLL), determined from observed and modelled pairs of activity at mass-depth. We estimated MSR variability from a heat map by plotting variability in NLL over a range of values for MSR and A_0 . We also estimated mean crab burrow depths using stratigraphic profiles of $^{210}\text{Pb}_{\text{xs}}$ and the modelling approach of McCraith et al. (2003). We estimated variability in mean crab burrow depth from a heat map by plotting variability in NLL over a range of values for mean crab burrow depth and burrow frequency.

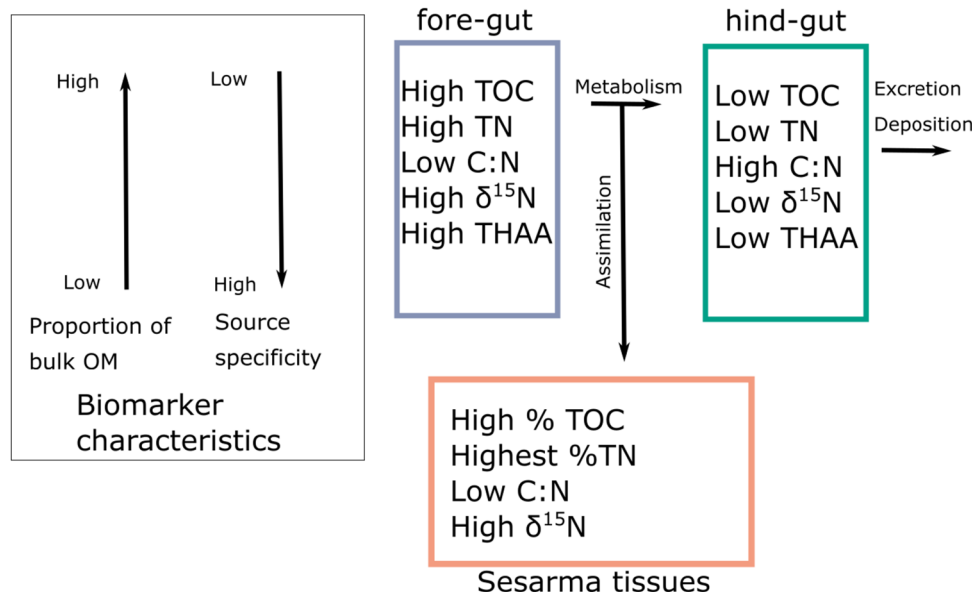
Sesarma and Sediment Sample Collection

The effects of *Sesarma* grazing on OM turnover were investigated by analyzing *Sesarma* gut contents, tissues, and marsh sediments for a suite of biomarkers, i.e., compounds that retain information about the sources and processing of OM. Some variables measured in this study are less source-specific but represent a larger fraction of the OM pool (e.g., elemental analysis, elemental ratios, stable isotopes), whereas amino acids are more source-specific but represent a smaller fraction of the total OM pool (Fig. 2). Samples for bulk geochemical analyses, including elemental and stable isotope analyses, were collected between 2017 and 2019 and are summarized in Table S1. Crab gut contents were analyzed to characterize changes in OM composition as it undergoes *Sesarma* processing. Whole *Sesarma* crabs and their tissues were collected in 2017, according to Prince et al. (2021) (Supplementary Methods), and analyzed for bulk geochemical values to evaluate trophic level enrichment. To identify *Sesarma* dietary sources, live *Spartina* leaves were collected and benthic diatoms were collected from the marsh and isolated for analysis at the University

of Florida, using methods similar to Borst et al. (2018) (Supplementary Methods). In 2019, crabs were collected from Sapelo Island, and gut samples were collected from the fore- and hind-guts of 175 individuals from three size classes (small (8.0–13.7 mm), medium (11.4–16.8 mm), and large (17.0–22.2 mm)). Fore- and hind-gut samples were composited based on sex and size classes (Table S2).

Sediment samples were collected in June 2018 from creek pairs (A–D) to evaluate differences in sediment OM between grazed and un-grazed creeks. Triplicate cores were collected in June 2018 from seven zones along each creek ($n = 168$ cores), using a push corer with a 10-cm-ID polycarbonate core barrel, and were sectioned in the field. Cores were inspected to determine if unconsolidated surface sediments (USS) were present. The soft and “fluffy” USS were distinguished from consolidated, root-bound sediment (hereafter referred to as “sediment”), which was denser and firmer. The USS was comprised of fine material, and if mussels were present, the USS could also contain their feces/pseudofeces. The USS was separated from the underlying sediment to evaluate differences between the recently deposited material (USS) and the deeper, root-bound material. If present, the thickness of the USS was measured, the core was extruded partially in a vertical position, and the USS was removed with a knife and transferred to a Whirl-pak™ bag. After the USS was collected, the underlying sediment was extruded and the topmost 5 cm of consolidated material was collected into a Whirl-pak™ bag. If no USS was present, the topmost (0–5 cm) sediment was collected. Samples were stored at 4 °C while in transit to the laboratory (< 4 h) and stored at –20 °C until further processing. Frozen samples were freeze-dried, homogenized, and ground with a roller mill prior to analysis.

Fig. 2 Summary schematic showing the *Sesarma*-driven mechanisms influencing marsh organic matter (OM) turnover and the biomarkers used to study *Sesarma* processes. Biomarkers are listed in order of source specificity, with bulk measures first, and more source specific biomarkers, such as THAA, listed last. THAA, total hydrolyzable amino acids; TOC, total organic carbon; TN, total nitrogen; C:N, Carbon:Nitrogen ratio



Bulk Geochemical Variables

A subset of the dried, ground samples (*Sesarma* gut contents, *Sesarma* muscle tissue, whole *Sesarma* crabs, *Spartina* leaf clippings, filtered diatom, USS and underlying consolidated sediments) were weighed into tin capsules for total carbon (TC), total nitrogen (TN), and $\delta^{15}\text{N}$ analysis, and another sample subset was weighed into silver capsules, fumigation-acidified according to Harris et al. (2001), and analyzed for total organic carbon (TOC) and $\delta^{13}\text{C}$. Elemental and stable isotope analysis was conducted at the University of Florida's Stable Isotope Laboratory, using a Carlo Erba 1500 CN elemental analyzer coupled to a Thermo Electron DeltaV Advantage isotope ratio mass spectrometer (Carlo Erba/Thermo Fisher Scientific™, Waltham, MA, USA). Stable isotope ratios for C and N are reported in standard delta notation ($\delta^{13}\text{C}$ and $\delta^{15}\text{N}$) relative to Vienna Pee Dee Belemnite (VPDB) and atmospheric N_2 , respectively. C:N is reported as the mass ratio, i.e., weight %TOC ÷ weight %TN. A two-endmember mixing model (Eq. 1) was used to evaluate the contribution of *Spartina* to the *Sesarma* diet, following the approach of Middelburg (2014), in which the $\delta^{13}\text{C}$ values of benthic diatoms and *Spartina* represent the carbon isotope ratios of the two primary food resources and the $\delta^{13}\text{C}$ value of *Sesarma* tissues represents the isotope value of the consumer.

$$\frac{(\delta^{13}\text{C}_{\text{Sesarma tissue}} - \delta^{13}\text{C}_{\text{Benthic diatoms}})}{(\delta^{13}\text{C}_{\text{Spartina leaves}} - \delta^{13}\text{C}_{\text{Benthic diatoms}})} \quad (1)$$

Amino Acid Biomarkers

Amino acids are the building blocks of proteins, can comprise 30–45% of the soil organic N pool (Stevenson 1994) and have been used to characterize OM and decomposition in numerous systems (Hutchings et al. 2018; Morrison et al. 2020; Aufdenkampe et al. 2001; Duan and Bianchi 2007; Henrichs and Farrington 1987; Ingalls et al. 2003; Lee et al. 2000; Wakeham and Lee 2019). They are effective markers of early diagenesis (Philben et al. 2016; Dauwe et al. 1999) and can provide insights into the specific compounds accumulated and metabolized by macroinvertebrates, which subsequently influences the compositional patterns of OM decay (Woulds et al. 2012). They are frequently evaluated collectively, as a “pool” of OM, and individually, as biomarkers of specific OM sources and processes. The entire hydrolyzable amino acid pool is referred to as total hydrolyzable amino acids (THAA), and high THAA values indicate relatively recent OM inputs. Freshness of the OM pool can be evaluated with the unitless amino acid degradation index (DI), described below. Amino acids can also

be used as biomarkers of OM source material, as some are either unique to, or found in much higher concentrations, in specific OM sources. For instance, diaminopimelic acid (DAPA), gamma-aminobutyric acid (GABA), and muramic acid (MurA) are used as indicators of bacterial contributions to the OM pool (Philben et al. 2016), whereas hydroxyproline (Hyp) is found only in the cell walls of higher plants and some algae, and thus can serve as a vegetation indicator (Philben et al. 2016; Philben and Benner 2013).

Sediment samples from one grazed and one un-grazed creek (all zones, Creek Pair A) and *Sesarma* crab gut contents (fore- and hind-gut) were analyzed for 19 amino acids, according to Hutchings et al. (2018), with a Thermo Scientific Dionex 3000™ ultra-high-performance liquid chromatography system, coupled to a Thermo Scientific TSQ Endura H-ESI triple quadrupole mass spectrometer (Thermo Fisher Scientific™, Waltham, MA, USA). Samples that contained amino acids in concentrations below detectable levels are noted in the data sheet in this project's GitHub repository. An amino acid degradation index (DI) was calculated according to Dauwe et al. (1999) and Philben et al. (2016) for each sample, using R version 4.0.0. The DI was calculated with Eq. 2, in which Var_i is the relative molar abundance of amino acid i in the sample, Avg_i is the mean, and SD_i is the standard deviation of the amino acid across the entire dataset, and PC1_i is the loading score of the amino acid on the first principal component. The DI provides a unitless measure of how fresh or degraded the OM pool is and is driven by loss of amino acids such as leucine (Leu), isoleucine (Ile), phenylalanine (Phe), tyrosine (Tyr) and histidine (His), and preferential accumulation of glycine (Gly) and threonine (Thr) during diagenesis (Philben et al. 2016; Dauwe et al. 1999; Dauwe and Middelburg 1998). In general, higher DI values indicate less degraded material, while lower DI values indicate greater degradation (Philben et al. 2016).

$$\text{DI} = \sum \left(\frac{\text{Var}_i - \text{Avg}_i}{\text{SD}_i} \right) \times \text{PC1}_i \quad (2)$$

Statistical Analysis and Data Accessibility

For gut samples, a Fisher F -test was first conducted to determine if variances were significantly different between fore- and hind-guts for each bulk measure (%TC, %TOC, %TN, $\delta^{13}\text{C}$, $\delta^{15}\text{N}$, C:N), total hydrolyzable amino acids (THAA), and the amino acid degradation index (DI). If variances were not significantly different, then a Welch two-sample t test was conducted to compare means. If variances were not equal, then a non-parametric Wilcoxon rank sum exact test was conducted. If the data had ties, i.e., values were the same rank, the Wilcoxon rank sum test was run with a

continuity correction. Sediment data were tested to see if they were normally distributed, and if not, they were analyzed with a non-parametric Kruskal Wallis (KW) test with a Dunn's multiple comparison post hoc test, using the R package Dunn's test (2017). Significant differences between grazed and un-grazed creek USS depths were assessed using a KW test, with USS depth as the response variable and creek type (grazed or un-grazed) as the grouping factor. Significant differences between grazed and un-grazed sediment THAA and DI were tested with a KW test. For sediment samples, a random effects model was run for each bulk measure (%TC, %TOC, C:N, $\delta^{13}\text{C}$, TN, and $\delta^{15}\text{N}$), with grazing status as the fixed, independent variable, and creek zone as the random effects term.

Availability Statement

Data from this paper are archived in the publicly available Environmental Data Initiative Data portal, with the following <https://doi.org/https://doi.org/10.6073/pasta/9f4f43b8bf95c28896fc1d8ef5f020b> (Morrison et al. 2022). Data and analysis scripts are also archived in the following public GitHub repository: https://github.com/elisemorrison/Sesarma_soils_manuscript.

Results

Radionuclides

Average inventories (dpm cm^{-2}) of ${}^7\text{Be}$ from Zone 3 and Zone 6 of the grazed creek sites (A, B) were larger than those from the un-grazed creeks (Fig. 3a), showing a greater flux of this atmospherically derived radionuclide to grazed creeks. The average ${}^7\text{Be}$ inventory in grazed creek A and grazed creek B were 1.7-fold and 2.1-fold greater than that of their un-grazed counterparts, respectively (Fig. 3a). The relative differences in ${}^7\text{Be}$ inventories for grazed and un-grazed creeks were greatest in the marsh platform (Zone 6) for both creek pairs. Although the maximum sediment depth at which ${}^7\text{Be}$ could be detected was similar at all core locations for a given core collection date (Fig. 3b), the average ${}^7\text{Be}$ inventory, and hence flux, was significantly greater in the grazed creeks compared to the un-grazed creeks.

The maximum sediment depth at which ${}^{210}\text{Pb}_{\text{XS}}$ could be measured was three- to sixfold greater in the location with greatest *Sesarma* grazing (i.e., 24 cm in grazed creek B Zone 3; Fig. 3c) compared to the other core sites for creek pair B, where it ranged from 4 to 8 cm. Likewise, the ${}^{210}\text{Pb}_{\text{XS}}$ inventory (Fig. 3d) at the same site (grazed creek B Zone 3) was approximately tenfold greater than at the other core sites in creek pair B and ~ threefold greater than the inventories found at core sites in creek pair A. The grazed

creek B Zone 3 inventory ($32.7 \pm 1.6 \text{ dpm cm}^{-2}$) was similar to the expected inventory for the region ($\sim 33 \text{ dpm cm}^{-2}$) (Baskaran et al. 1993).

Radionuclides indicated that apparent sediment accretion rates and estimated mean burrow depths were greatest at the site with the most active *Sesarma* burrowing (i.e., grazed creek B Zone 3), compared to other sites. Apparent accretion rates (Fig. 3e) were 10 to 20-fold greater at this site (0.42 cm yr^{-1}) relative to the other sites from creek pair B ($0.02\text{--}0.04 \text{ cm yr}^{-1}$) and were ~ threefold greater than accretion rates from all sites in creek pair A ($0.12\text{--}0.14 \text{ cm yr}^{-1}$). Estimated mean burrow depth was also greatest at this site (50 cm; Fig. 3f), whereas estimated mean burrow depth was $< 1 \text{ cm}$ at other sites in creek pair B (with no *Sesarma* burrows present), and all sites from creek pair A had estimated mean burrow depths of 11–21 cm. Considering all cores, the ${}^{210}\text{Pb}_{\text{XS}}$ inventory was positively correlated to mean burrow depth ($n=8$, $r=0.96$, Fig. 3h).

Bulk Geochemical Variables: Endmembers

Endmembers (*Sesarma* gut contents, muscle tissue, whole *Sesarma* crabs, *Spartina* leaf clippings and filtered diatoms) were assessed for bulk geochemical variables to provide insights into OM transformations following consumption by *Sesarma*. There was little difference in bulk measures between *Sesarma* sex and size classes (Table S2), and results from both groups were pooled. There were significant changes in bulk C and N measures as OM passed from *Sesarma* fore-guts to hind-guts. In general, TC, TOC, TN, and $\delta^{15}\text{N}$ declined from the fore- to hind-guts, whereas C:N and $\delta^{13}\text{C}$ increased from the fore- to hind-gut. Specifically, from fore- to hind-guts, %TC declined from 37 to 20% (Wilcoxon exact test, $p < 0.05$), TOC declined from 36 to 20% (Wilcoxon test with continuity correction, $p < 0.05$), and %TN declined from 5.2 to 1.0% (Wilcoxon test with continuity correction, $p < 0.05$), indicating *Sesarma* C and N uptake between their fore- and hind-guts. From fore- to hind-gut, $\delta^{15}\text{N}$ values decreased from 6.16 to 5.39‰ (0.77‰ decline; Wilcoxon test with continuity correction, $p < 0.05$), likely driven by N metabolism. Between fore- and hind-guts, C:N increased from 7.24 to 21.01 (Wilcoxon exact test, $p < 0.05$), and $\delta^{13}\text{C}$ rose slightly, from -15.4 to $-15.1\text{\textperthousand}$ ($p < 0.05$) (Fig. 4, Table S2), likely driven by *Sesarma* C uptake as OM traversed their guts.

The contribution of *Spartina* to *Sesarma* diets was evaluated with a two-endmember mixing model that incorporated $\delta^{13}\text{C}$ values of *Sesarma* tissues and their two primary food sources, *Spartina* and benthic diatoms (Eq. 1). *Spartina* had a C:N of 23.3, a $\delta^{15}\text{N}$ value of 3.81‰ (± 0.11), and a $\delta^{13}\text{C}$ value of $-13.79\text{\textperthousand}$ (± 0.43), whereas benthic diatoms had a C:N of 11.8 (± 0.4), a $\delta^{15}\text{N}$ value of 2.73‰ (± 0.5), and $\delta^{13}\text{C}$ value of $-19.55\text{\textperthousand}$ (± -0.9) (Figs. 4, 5 and Table S2). The

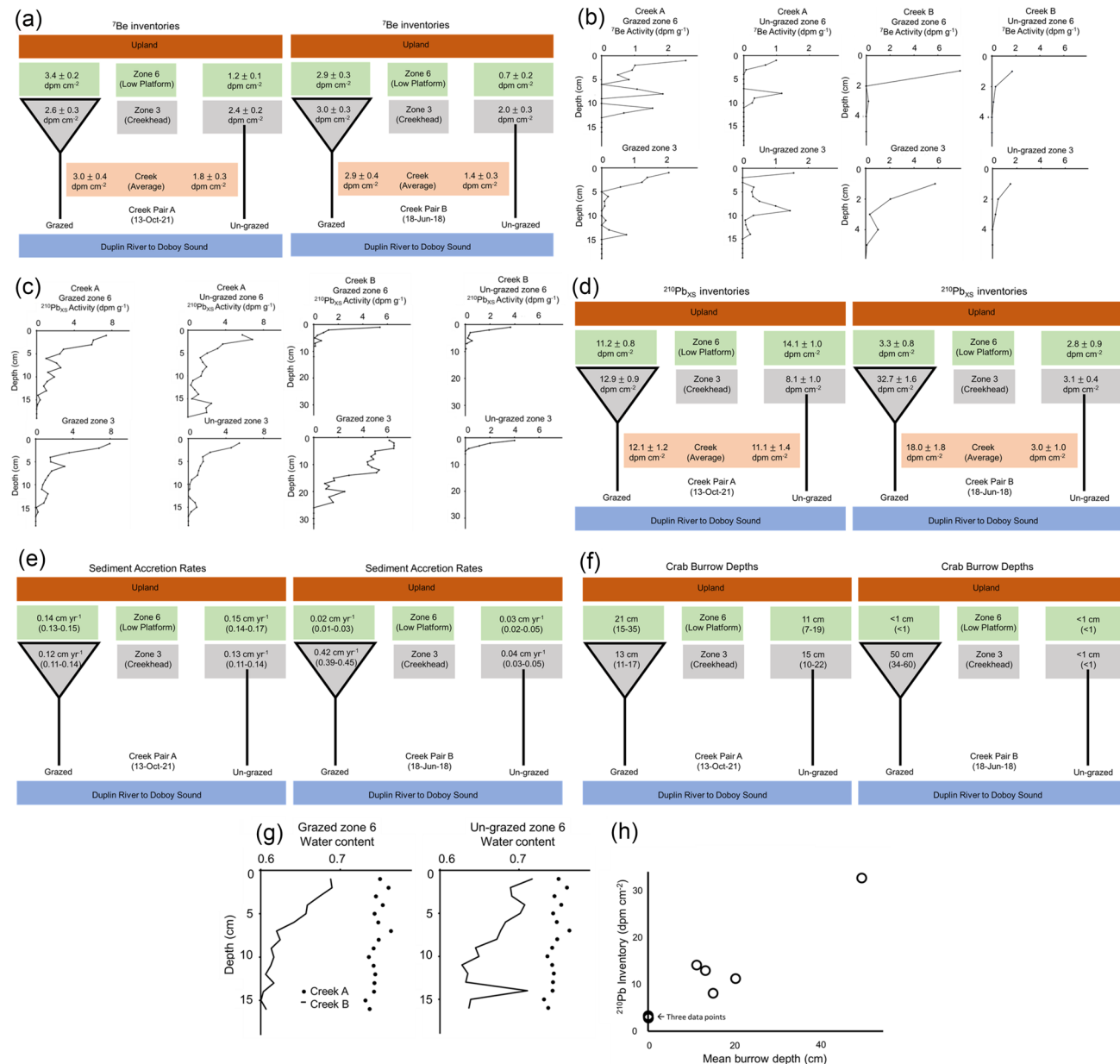


Fig. 3 Radionuclide data from creek pairs A and B. **a** ${}^7\text{Be}$ inventories (dpm cm^{-2}) for sediment cores collected at creek pair A (13-Oct-21) and creek pair B (18-Jun-18). **b** ${}^7\text{Be}$ activities (dpm g^{-1}) plotted against the maximum depth of the sediment interval for sediment cores collected at creek pair A (left) and creek pair B (right). **c** ${}^{210}\text{Pb}_{\text{XS}}$ activities (dpm g^{-1}) plotted against the maximum depth of the sediment interval for sediment cores collected at creek pair A (left) and creek pair B (right). **d** ${}^{210}\text{Pb}_{\text{XS}}$ inventories (dpm cm^{-2}) presented for sediment cores collected at creek pair A and creek pair B. **e** Sediment accretion rates determined with ${}^{210}\text{Pb}_{\text{XS}}$ activities using the constant-flux, constant-sedimentation model (Krishnaswamy et al. 1971) presented for sediment cores collected at creek pair A and creek pair B. **f** Mean crab burrow depths (cm) determined with ${}^{210}\text{Pb}_{\text{XS}}$ activities and the modelling approach of McCraith et al. (2003) presented for sediment cores collected at creek pair A and creek pair B. **g** Comparison of fraction wet weight (i.e., porosity) for creek A (dark circles) and creek B (dark line). These plots show a cm-by-cm (0–16 cm, n=16) comparison (creek A vs. creek B) of fraction wet weight for cores collected in Zone 6 (low platform). **h** Mean burrow depth (cm) determined from the stratigraphic profiles of ${}^{210}\text{Pb}_{\text{XS}}$ plotted against excess ${}^{210}\text{Pb}$ inventory (dpm cm^{-2}) for each of eight cores

mixing model indicated that 90.8% of the C in *Sesarma*'s diet was derived from *Spartina*, with the remaining 9.2% derived from benthic diatoms. Additionally, the increase in ${}^{15}\text{N}$ between *Spartina* leaves and *Sesarma* tissues, as well

et al. 1971) presented for sediment cores collected at creek pair A and creek pair B. **f** Mean crab burrow depths (cm) determined with ${}^{210}\text{Pb}_{\text{XS}}$ activities and the modelling approach of McCraith et al. (2003) presented for sediment cores collected at creek pair A and creek pair B. **g** Comparison of fraction wet weight (i.e., porosity) for creek A (dark circles) and creek B (dark line). These plots show a cm-by-cm (0–16 cm, n=16) comparison (creek A vs. creek B) of fraction wet weight for cores collected in Zone 6 (low platform). **h** Mean burrow depth (cm) determined from the stratigraphic profiles of ${}^{210}\text{Pb}_{\text{XS}}$ plotted against excess ${}^{210}\text{Pb}$ inventory (dpm cm^{-2}) for each of eight cores

as the C:N values, confirmed that *Sesarma* largely consume *Spartina*, and gut analyses indicated that the OM content and quality of this plant material is altered significantly as it is processed in the gut of this keystone engineer.

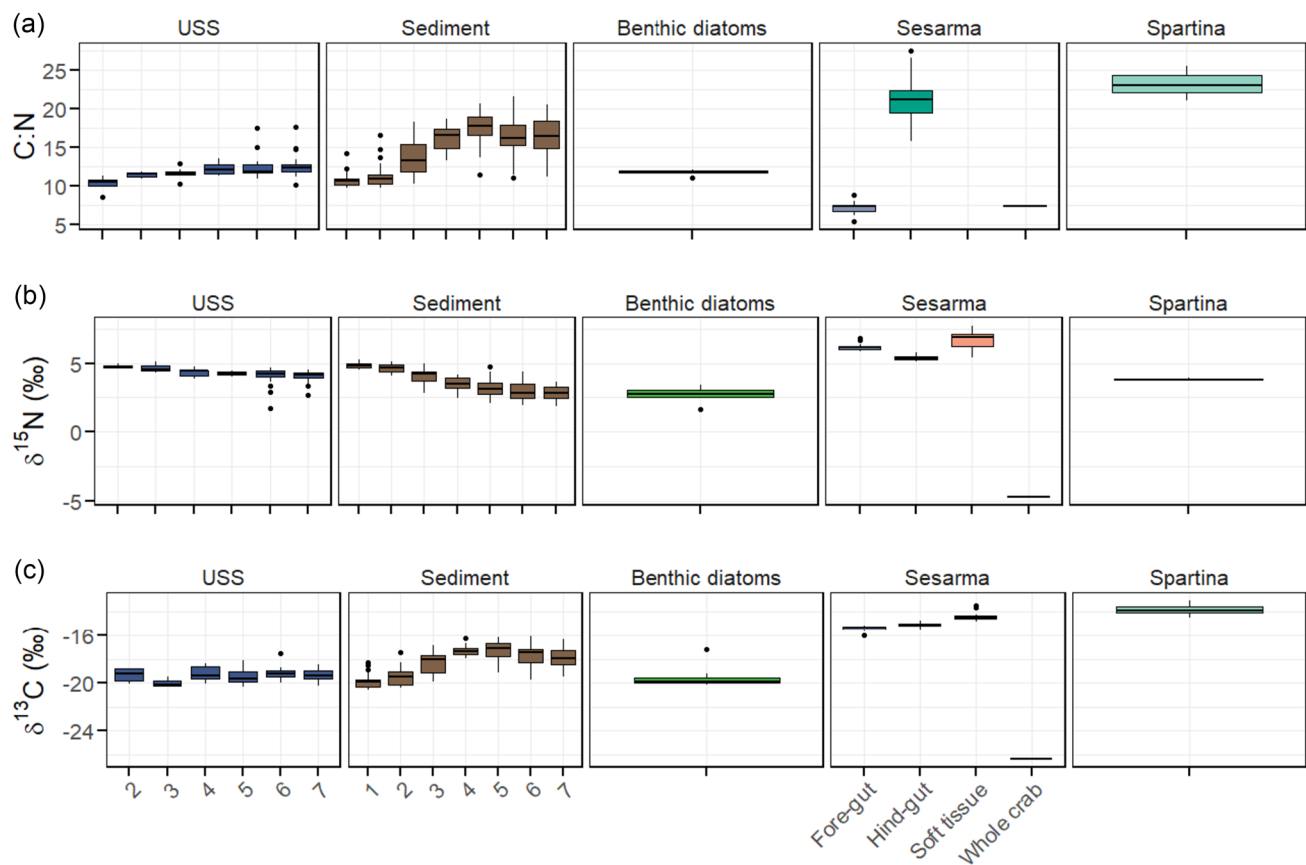
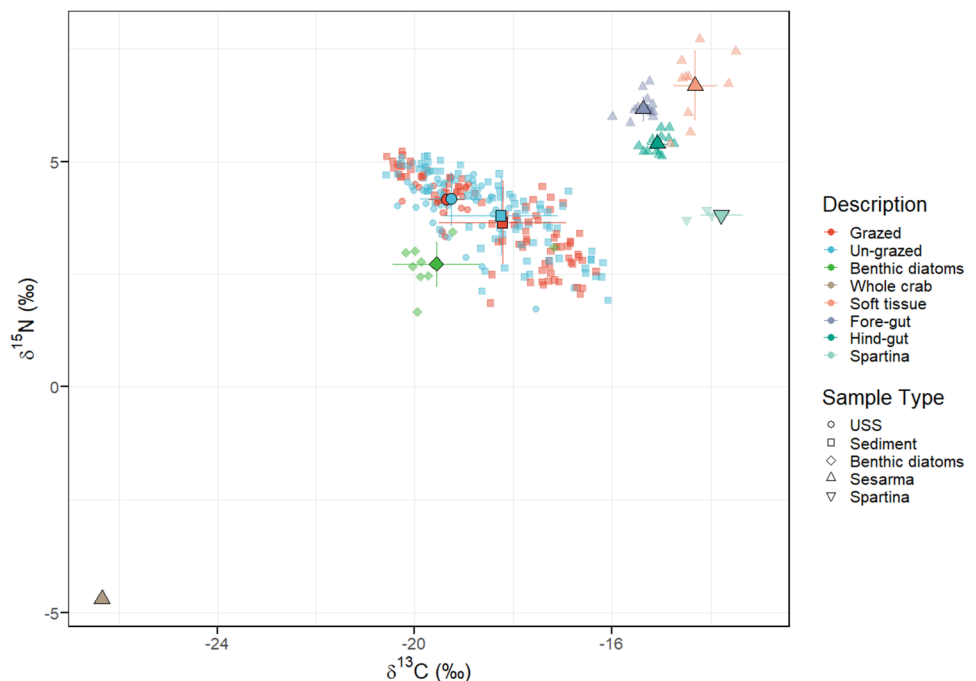


Fig. 4 Bulk geochemical variables for sediments and unconsolidated surficial sediment (USS) along each creek zone (with grazed and ungrazed creek data combined) and for endmembers (diatoms, *Sesarma*, and *Spartina* leaves). **a** Carbon: Nitrogen (C:N) ratios increased from the sound (Zone 1) to the marsh platform (Zones 6 and 7), and

increased from *Sesarma* fore- and hind-guts. **b** Stable isotope values of nitrogen ($\delta^{15}\text{N}$) decreased from the sound (Zone 1) to the marsh platform (Zones 6 and 7) and decreased from *Sesarma* fore- to hind-guts. **c** Stable isotope values of carbon ($\delta^{13}\text{C}$) increased from the sound (Zone 1) to the marsh platform (Zones 6 and 7)

Fig. 5 Stable isotope values for all sample types and endmembers. Sample types separated into distinct clusters based on their $\delta^{13}\text{C}$ and $\delta^{15}\text{N}$ values. The whole crab sample plots separately from other samples because it included homogenized crab carapace, guts, and tissues. USS, unconsolidated surface sediment



Bulk Geochemical Variables: USS and Sediments

To evaluate *Sesarma*'s influence on sediment OM, bulk geochemical variables were measured for both the unconsolidated surface sediment (USS) and underlying, firmer sediments. There were marked differences between variables measured in USS and bulk sediment between grazed and un-grazed creeks. USS was present in only the low- and high-marsh platform sites of the grazed creeks (2 of 7 zones) but was encountered in 6 of the 7 zones in un-grazed creeks (Fig. S1; Table S3). The thickness of the USS layer was also significantly greater in un-grazed creeks (KW and Dunn's Test, $p < 0.05$), with the thickest USS layers occurring adjacent to the creek head (Zone 4, 1.7 ± 0.8 cm) and on the low- and high-marsh platforms (Zone 6, 1.7 ± 0.9 cm; Zone 7, 1.7 ± 1 cm; Fig. S1), likely a consequence of slower flow rates in the un-grazed creeks (Ortals et al. 2021).

Among all bulk measures for USS and underlying consolidated sediments, we observed high inter-creek differences, which were particularly pronounced in the firm sediments (Fig. S2). High inter-creek variability is likely a consequence of differences in site history, duration and stage of grazing succession, and hydrology—factors that likely mask some differences when data are aggregated across creeks (Fig. S2). Because of the lack of USS in grazed creeks, there was insufficient replication of bulk measures on USS samples to run statistical analyses (Table S4).

Relative to USS, underlying sediments generally had greater C:N, %TC, and $\delta^{13}\text{C}$ values, and lower $\delta^{15}\text{N}$ values, indicating a greater contribution of C_4 marsh vegetation to the deeper sediment pool (likely *Spartina*; typical values around $-13\text{\textperthousand}$; this paper; (Currin et al. 1995; Baker et al. 2013)) (Figs. 4 and 5). A random effects model indicated that sediment C measures (%TC, %TOC, C:N, and $\delta^{13}\text{C}$) did not differ significantly between grazed and un-grazed creeks ($p \geq 0.1$), which may be a consequence of high inter-creek variability, a lag in the effect of grazing on bulk measures, or a change in C composition, but not quantity, between grazed and un-grazed creeks. In contrast, sediment N measures, specifically $\delta^{15}\text{N}$ and %TN, exhibited significant ($p = 0.03$) and marginally significant ($p = 0.08$) differences between grazed and un-grazed creeks, respectively. Grazed creeks had lower $\delta^{15}\text{N}$ values than un-grazed creeks ($3.65 \pm 0.9\text{\textperthousand}$ vs $3.8 \pm 0.8\text{\textperthousand}$, respectively; Fig. 4). Grazed creeks had marginally greater %TN than un-grazed creeks, with the greatest mean %TN (0.43 ± 0.1) occurring in the marsh zones directly adjacent to the grazing front (Zones 5–7) of the grazed creeks (Fig. 3; Table S5).

Amino Acids

Total Hydrolyzable Amino Acids (THAA) and the Degradation Index (DI)

To evaluate how the bulk amino acid pool was altered by *Sesarma* digestive processes, we analyzed total hydrolyzable amino acids (THAA) and the amino acid degradation index (DI) in fore- and hind-gut samples and compared them with sediment samples from grazed and un-grazed creeks. Both THAA and the DI were significantly different between samples from *Sesarma* fore- and hind-guts. The *Sesarma* fore-guts had significantly greater THAA concentrations (Wilcoxon exact test, $p < 0.05$), indicating a loss in THAA from fore- to hind-guts. *Sesarma* fore-guts also had significantly lower DI values than the hind-guts (Wilcoxon exact test, $p < 0.05$; Table S6). This was contrary to our expectations, as the DI indicated that *Sesarma* fore-guts had the most degraded (i.e., lowest DI) material, while hind-guts had slightly fresher material (i.e., intermediate DI), and that sediments had the freshest material (i.e., greatest DI). However, for this dataset, the DI should be interpreted with caution, as the DI is calculated based on the loadings of each amino acid on the first principle component of a PCA, and the directionality of the loading score of some of our amino acids (including Leu and Phe) did not show the expected directionality seen in other studies (Philben et al. 2016) (Table S6). As with bulk measures, there was insufficient replication of USS samples to test for significant differences in THAA or DI between USS from grazed and un-grazed creeks. For sediment samples, there was no significant difference in either THAA or DI between grazed and un-grazed creeks (KW and Dunn's Test; THAA, $p = 0.2$ and DI, $p = 0.1$), likely because of inter-creek variability and the influence of multiple source inputs of amino acids.

Amino Acid Biomarkers

To evaluate how specific amino acids such as bacterial and vegetation markers are altered by *Sesarma*, we compared source-specific amino acids between fore- and hind-guts, and between grazed and un-grazed-creek sediments. There were no significant differences in the concentrations of bacterial markers (MurA, DAPA) and the vegetation marker Hyp (Wilcoxon test, $p > 0.05$) between *Sesarma* fore- and hind-guts. However, the concentration of all other amino acids (15 of 19), including glutamic acid (Glu), declined significantly from *Sesarma* fore-guts to hind-guts (Fig. 6).

When we compared source-specific amino acids between grazed and un-grazed creeks, we found that bacterial markers were greater in un-grazed USS, and that vegetation

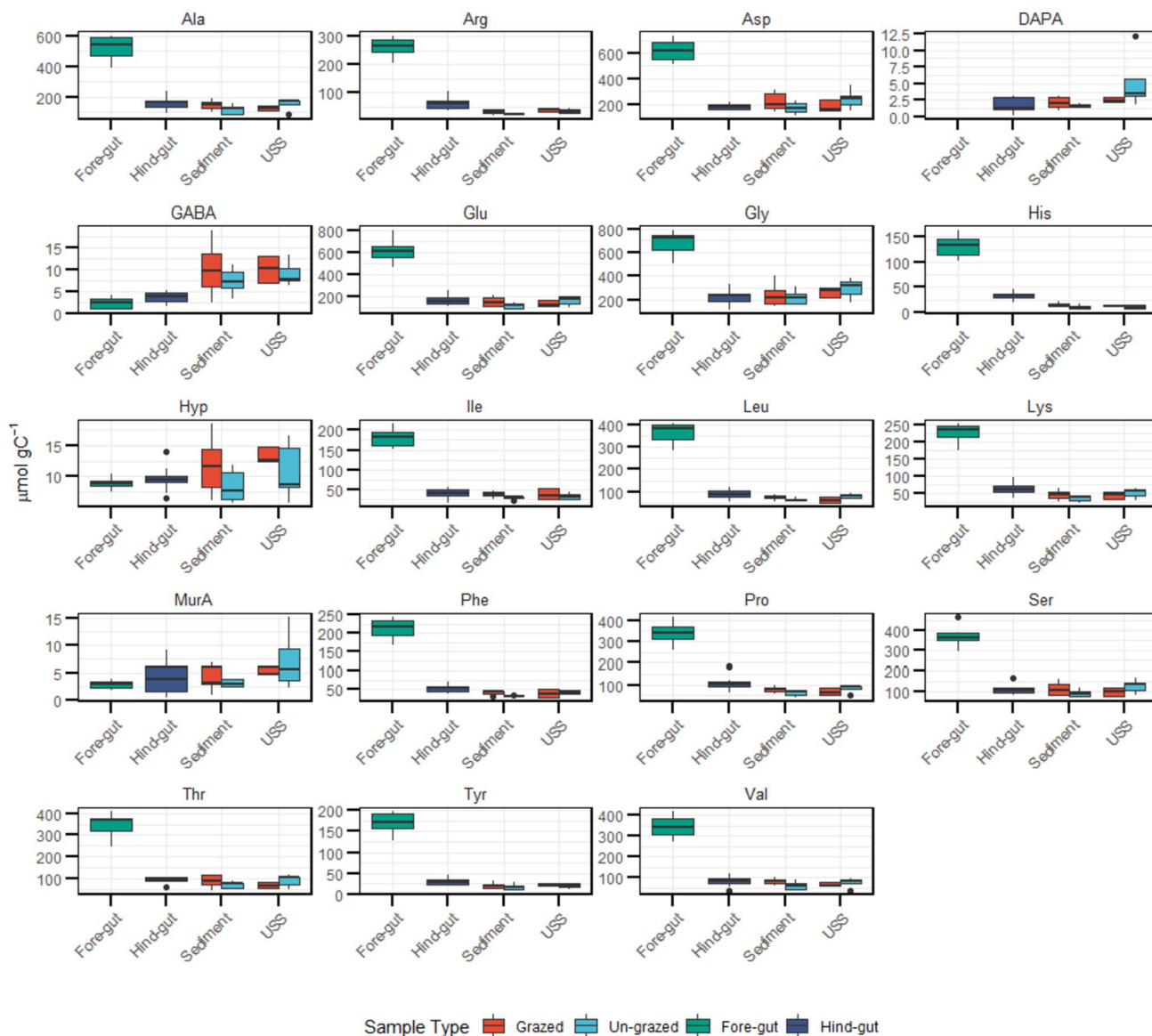


Fig. 6 Amino acids measured for *Sesarma* fore- and hind-guts and grazed (red) and un-grazed (blue) sediment and unconsolidated surface sediment (USS). Most amino acids were greatest in *Sesarma* fore-guts (green) and declined considerably between fore- and hind-guts, indicating assimilation or metabolic loss. The only amino acids that did not exhibit this trend were source-specific amino acids, such as Hyp (vegetation biomarker), GABA and MurA (bacterial bio-

markers). Ala, alanine; Arg, arginine; Asp, aspartic acid; DAPA, diaminopimelic acid; GABA, gamma aminobutyric acid; Glu, glutamic acid; Gly, glycine; His, histidine; Hyp, hydroxyproline; Ile, isoleucine; Leu, leucine; Lys, lysine; MurA, muramic acid; Phe, phenylalanine; Pro, proline; Ser, serine; Thr, threonine; Tyr, tyrosine; Val, valine

markers were greater in grazed-creek sediments, suggesting differences in OM sources between creek types. Specifically, relative to the grazed-creek USS, the un-grazed-creek USS had greater concentrations of bacterial amino acids DAPA and MurA (Table S6), as well as greater concentrations of alanine (Ala), aspartic acid (Asp), glutamic acid (Glu), glycine (Gly), serine (Ser), leucine (Leu), and valine (Val;

Table S6; Fig. 6). The grazed-creek sediments had marginally greater concentrations of the vegetation marker Hyp than the un-grazed-creek sediments (KW and Dunn's Test; $p=0.08$), but there was no significant difference in the concentrations of bacterial amino acids DAPA (KW, $p=0.33$) and MurA (KW, $p=0.39$) between sediments of the grazed and un-grazed creeks (Fig. S3).

Discussion

Sesarma directly alter marsh sedimentation and OM cycling through their grazing and burrowing activities in Georgia salt marshes. Inventories and depth distributions of radio-nuclides ^{210}Pb and ^7Be indicated greater bioturbation and longer periods of tidal inundation in *Sesarma*-grazed creeks when compared with un-grazed creeks. Biomarkers indicated that *Sesarma*'s digestive processes alter the concentrations and stable isotope values of OM in grazed creek sediments, and the stable isotope values of *Sesarma* food sources and tissues indicated that *Spartina* is the primary food source for this crab. These multiple lines of evidence confirm that *Sesarma* burrowing and grazing influence marsh sediment characteristics and OM turnover in salt marshes of the Southeastern USA.

Linkages Between *Sesarma* Burrowing Depths and Sediment Mixing

Although fiddler crabs can affect *Spartina* growth (Martínez-Soto and Johnson 2023), *Sesarma* can excavate more sediment, increase plant mortality, and elongate creeks relative to other common burrowing crabs, including fiddler crabs (Vu and Pennings 2021; Vu et al. 2017). To evaluate *Sesarma* burrowing at our sites, we applied the modelling approach of McCraith et al. (2003) to estimate burrow depths using $^{210}\text{Pb}_{\text{xs}}$ stratigraphies in grazed and un-grazed creeks. The site with the most active *Sesarma* burrowing had an estimated mean burrow depth of 50 cm, which was much greater than other sites in creek pair B (< 1 cm), and greater than all sites in creek pair A (11–21 cm). The high estimated mean burrow depth from this site was slightly greater than maximum reported value (40 cm) for *Sesarma* burrows in New England marshes (Bertness et al. 2009), and twice the maximum value (25 cm) reported for fiddler crab (*Uca* spp.) burrows in marshes of South Carolina (McCraith et al. 2003). Both the depth of detection of $^{210}\text{Pb}_{\text{xs}}$ and the corresponding estimated burrow depth indicate that *Sesarma* have the potential to excavate marsh sediments (and thus irrigate and oxidize sediments) to a greater vertical extent than fiddler crabs.

Additionally, we found that the zone with the most active *Sesarma* burrowing (grazed creek B, Zone 3) had $^{210}\text{Pb}_{\text{xs}}$ to a depth of 24 cm—more than three times deeper than sites without burrowing and 1.5-fold deeper than sites with only fiddler crab burrowing. Likewise, at this same site, the CFCS model indicated a mean marsh accretion rate of 0.42 cm yr^{-1} , far greater than what is expected in salt marshes from this area (Crotty et al. 2020). In this case, however, it is likely that the apparent accretion rate is greater than the true accretion rate because of sediment burrowing by *Sesarma*.

Insights into Bioturbation and Sediment Inundation with $^{210}\text{Pb}_{\text{xs}}$ and ^7Be Sediment Stratigraphies and Inventories

Not only did *Sesarma*-grazed creeks have deeper estimated burrow depths relative to their un-grazed counterparts, but they also exhibited indications of greater tidal inundation. This is in agreement with past findings that *Sesarma*'s ability to alter salt marsh drainage and morphology is enhanced by recent sea level rise (Crotty et al. 2017; Hughes et al. 2009; Angelini et al. 2018). Marsh drainage ratios are defined as the marsh area divided by the length of the creek that drains the area. Marshes with high drainage ratios experience longer periods of tidal inundation because more time is needed for the creek to drain the water delivered to the marsh during high tides. Longer periods of tidal inundation soften marsh sediments, making it easier for crabs to burrow (Bertness et al. 2009), thus *Sesarma* favor creeks with greater drainage ratios (Crotty et al. 2020). With a longer duration of seawater inundation during a tidal cycle, a marsh with a greater drainage ratio should also receive greater $^{210}\text{Pb}_{\text{xs}}$ delivery from seawater. Such protracted inundation results in a longer marsh residence time for $^{210}\text{Pb}_{\text{xs}}$, giving fine particles and their adsorbed $^{210}\text{Pb}_{\text{xs}}$ more time to settle. This process likely contributes to greater accumulation of $^{210}\text{Pb}_{\text{xs}}$ in the grazed creek relative to un-grazed creek for creek pair B. If *Sesarma*-grazed creeks have greater drainage ratios than un-grazed creeks, then we would expect sediment stratigraphies from *Sesarma*-grazed creeks to show greater $^{210}\text{Pb}_{\text{xs}}$ inventories (dpm cm^{-2}) than un-grazed creeks, which indeed, is what we found. The $^{210}\text{Pb}_{\text{xs}}$ inventory at the site with active *Sesarma* grazing and burrowing was approximately sevenfold greater than $^{210}\text{Pb}_{\text{xs}}$ inventory in the un-grazed creek, which further demonstrates that *Sesarma* favor creeks with greater drainage ratios and that *Sesarma* burrowing influences the deposition and net accumulation of $^{210}\text{Pb}_{\text{xs}}$.

If, however, we assume that *Sesarma* bioturbation does not enhance $^{210}\text{Pb}_{\text{xs}}$ accumulation at the site with active *Sesarma* grazing and burrowing, and we accept the CFCS model estimate of sedimentation, then the greater $^{210}\text{Pb}_{\text{xs}}$ inventory found at this site could simply be explained by a high sedimentation rate. But the CFCS model estimate of sedimentation at this site is more than threefold greater than at the other sites in this study and is much larger than the values from similar areas in other studies (Crotty et al. 2020). Considering this, and given our visual confirmation of intense *Sesarma* burrowing at this location, we attribute the larger $^{210}\text{Pb}_{\text{xs}}$ inventory and $^{210}\text{Pb}_{\text{xs}}$ penetration depth to *Sesarma* bioturbation and the longer tidal inundation times associated with *Sesarma* grazing in creek pair B. Interpretation of the $^{210}\text{Pb}_{\text{xs}}$ inventories for creek pair A, however, was

ambiguous, as there was no apparent pattern with respect to *Sesarma* grazing or creek location. These results illustrate the challenges associated with interpreting radionuclide data from sites with complex and dynamic sedimentation, like salt marshes (Arias-Ortiz et al. 2018). Nevertheless, across all eight cores, estimated mean burrow depth (*Sesarma* or *Uca*) was strongly correlated ($r=0.96$, $n=8$) with $^{210}\text{Pb}_{\text{XS}}$ inventory (Fig. 3h), and results from creek pair B strongly suggest that *Sesarma* influence $^{210}\text{Pb}_{\text{XS}}$ stratigraphy.

^{7}Be as an Indicator of Hydraulic Exchange Capacity

Crotty et al. (2020) suggested that *Sesarma* grazing of marsh creeks is a self-attenuating process. *Sesarma* favor creeks with a larger drainage ratio, but as *Sesarma* grazing fronts move landward and creeks lengthen, they reduce the drainage ratio and increase the hydraulic exchange capacity of the creek, i.e., the ability of the creek to drain the associated marsh. This enhanced hydraulic exchange capacity eventually makes creeks unsuitable for further *Sesarma* grazing (Crotty et al. 2020; Vu and Pennings 2021). After this occurs, *Spartina* can revegetate the previously denuded mudflat, leaving a narrow band of burrowed marsh at the creek head (Crotty et al. 2020). Additionally, crabs can move to un-grazed creeks with a lower hydraulic exchange capacity, where the process can repeat.

We found that ^{7}Be inventories serve as an indicator of the hydraulic exchange capacity in creeks. The average ^{7}Be inventory at both grazed creeks was greater than inventories at un-grazed creeks, suggesting that during the ~9 months preceding core collection, *Sesarma*-grazed creeks experienced longer periods of tidal inundation than the un-grazed creeks. The greater inventory of ^{7}Be in grazed-creek sediments was likely driven, in part, by the greater drainage ratio and lesser hydraulic exchange capacity of the grazed creeks, which led to a longer residence time for tidally delivered ^{7}Be , and more time for ^{7}Be -associated particle deposition in the grazed creek. Crab burrows also provide effective conduits for ^{7}Be infiltration into the sediments and likely contributed to greater ^{7}Be inventories in grazed creeks. In creek pair A, estimates of mean burrow depth were similar in the grazed and un-grazed creeks (both zones), but the average ^{7}Be inventory was 1.7-fold greater in the grazed creek, compared to the un-grazed creek. Likewise, estimated mean burrow depths were <1 cm for both grazed and un-grazed creeks in creek pair B, zone 6, but the ^{7}Be inventory was 4.1-fold greater in the grazed creek. Consideration of both ^{7}Be inventories and estimated mean burrow depths from creek pair A (both zones) and creek pair B (zone 6) indicates that hydraulic exchange capacity and duration of tidal inundation influence ^{7}Be inventories. Comparison of ^{7}Be inventories between the grazed and un-grazed creeks suggests that at the time of core collection,

the hydraulic exchange capacity in the grazed creek was sufficiently low to maintain the tidal inundation required for continued *Sesarma* grazing and further creek incision. This finding supports prior conclusions that *Sesarma*-grazed creeks have greater drainage ratios than un-grazed creeks (Crotty et al. 2020) and highlight that ^{7}Be can serve as a useful indicator of the degree of hydraulic exchange capacity in creeks.

Digestive Processing of OM by *Sesarma* and Its Impact on Bulk Sediment Chemistry

In addition to finding changes in bioturbation and sediment inundation between grazed and un-grazed creeks, we also found that *Sesarma* influences salt marsh OM processing. Our simple two-endmember mixing model indicated that most of *Sesarma*'s diet was comprised of *Spartina*, and biomarker analyses showed that *Sesarma* digestive processes degraded *Spartina* OM, resulting in a significant reduction in C and N. Total C and N concentrations and stable isotope values, along with amino acid biomarkers, all indicated that this crab uptakes C and N between its fore- and hind-gut. From fore- to hind-gut, both %TC and %TOC dropped by nearly half, %TN exhibited an ~80% decrease, and the C:N ratio exhibited a ~threefold increase (Fig. 4), reflecting OM breakdown and selective assimilation of C and N, likely facilitated by endogenous enzymes secreted in their mid-gut (Linton 2020). Correspondingly, TC and TN values of *Sesarma* tissue were greater than in the fore-gut, and far greater than in the hind gut (Fig. 4 and Table S2), further indicating C and N uptake and storage in *Sesarma* tissues.

Stable isotopes provided further insights into *Sesarma* dietary sources and mechanisms of OM processing (Figs. 4 and 5). There was a 2.88‰ increase in $\delta^{15}\text{N}$ values between *Spartina* leaves and *Sesarma* tissues, similar to previously reported increases in $\delta^{15}\text{N}$ values between mangrove leaves and other sesarmid crab tissues (Kristensen et al. 2010), and similar to the global average of $2.2 \pm 0.30\text{‰}$ increase between plants and the herbivores that consume them (McCutchan et al. 2003). This trophic level enrichment indicated that *Spartina* is the principal food source for *Sesarma*, which was further supported by a two-endmember $\delta^{13}\text{C}$ mixing model that indicated 90.8% of the crab diet is derived from *Spartina*. Thus, differences in both $\delta^{13}\text{C}$ and $\delta^{15}\text{N}$ values between *Spartina* and *Sesarma* tissues indicate that the crabs consume *Spartina* as their primary food source. Additionally, invertebrates that consume low-N food (i.e., diets with high C:N, such as *Spartina*) do not discriminate as much against ^{15}N , resulting in greater retention of ^{15}N in their tissues (Jardine et al. 2005; Adams and Sterner 2000) and excretion of isotopically lighter ^{14}N (McCutchan et al. 2003; Gannes et al. 1998; Herbon and Nordhaus 2013), which was also observed here.

This ^{15}N -depleted material from *Sesarma* guts is likely deposited throughout the creek head via crab defecation and bioirrigation (increased exchange with overlying water through burrows), which can be an important driver of sediment biogeochemistry (Aller 1980; Zhang et al. 2019; Gilbert et al. 2003). This was supported by the significantly lower $\delta^{15}\text{N}$ value of grazed-creek sediments, as well as significantly greater %TN in grazed- versus un-grazed-creek sediments. A difference of 1‰ in bulk $\delta^{15}\text{N}$ values can indicate differences in trophic processes (Kristensen et al. 2010); thus, the differences in $\delta^{15}\text{N}$ between grazed and un-grazed creeks suggest *Sesarma* contributions to N turnover in the system. Values of $\delta^{15}\text{N}$ and %TN were particularly extreme in creek zones that exhibited the greatest burrow density (Fig. 4). Additionally, the degradation of amino acids through *Sesarma* digestive processes further indicated that grazing *Sesarma* facilitate N turnover, since amino acids can comprise 30–45% of soil organic N (Stevenson xxxx). Although beyond the scope of this study, *Sesarma* activities, such as burrowing and bioirrigation, may influence other salt marsh invertebrates and microbial communities. However, it is worth noting that the $\delta^{15}\text{N}$ values of *Sesarma* hind-guts did not match exactly those of the grazed-creek sediments, indicating there are likely other N sources and/or biogeochemical processes that contribute to the $\delta^{15}\text{N}$ value of creek sediments. For example, other faunal activity may play a role, or benthic diatom growth may be favored in light-replete grazing fans, which have increased in area since 2006 (Table S7) and may further contribute to the lower $\delta^{15}\text{N}$ values in grazed-creek sediments. Additional investigations into interactive effects among *Sesarma* grazing and marsh microbial communities are warranted, particularly considering that invertebrate OM processing can significantly modify sediment microbial assemblages (Dale et al. 2019).

Amino Acids and *Sesarma* OM Processing

Changes in amino acids between fore- and hind-gut samples also indicated N-rich amino acid uptake by the crabs. The fore-guts had significantly greater concentrations of THAAs than hind-guts, which had THAA concentrations within the range of sediment samples (Table S6). The significant decline in concentration for the majority (15 of 19) of amino acids, notably including the canonical trophic amino acid, glutamic acid (Glu; (Mayer et al. 1995)), indicated that many amino acids are removed (likely degraded or assimilated) between the *Sesarma* fore- and hind-gut. In invertebrates, uptake mechanisms can differ between amino acids, and some, such as Tyr, are passively absorbed, while others, such as Methionine, are taken up through active uptake (Self et al. 1995). Additionally, invertebrates can show plasticity in their enzymatic response to different

food sources (Bock and Mayer 1999), although few studies have evaluated changes in amino acids specifically through *Sesarma* guts. However, Woulds et al. (2012) found that Phe, Val, Leu, Ile, Thr, and Pro accumulate in polychaete tissues, and that Lys, Asp, and Glu are lost rapidly through metabolism. As OM passes from *Sesarma*'s fore-gut to hind-gut, metabolic processes may affect these amino acids similarly. Because amino acids comprise a large fraction of the organic N pool, this finding highlights that *Sesarma* are consuming and assimilating N-rich, fresh OM, likely derived from *Spartina*.

Bacterial extracellular proteolytic activity can also play an important role in intertidal sediment N cycling (Mayer 1989). The amino acids DAPA and MurA are both bacterial cell wall markers (Hutchings et al. 2018; Morrison et al. 2020; Philben et al. 2016) and exhibited greater concentrations in USS samples, as well as in grazed-creek sediments. The higher concentrations in USS suggest that microbial biomass may be greater in USS samples. USS layers were thicker in un-grazed creeks, likely caused by the high density of mussels (Angelini et al. 2015, 2018) and their feces and pseudofeces (Smith and Frey 1985) in un-grazed creek heads. We also found that concentrations of the vegetation marker Hyp were marginally greater in grazed creeks than in un-grazed creeks. Hydroxyproline (Hyp) is a component of plant cell walls and some algae and has been used to evaluate the contributions of vegetation to soil organic N, and has been seen to increase with *Spartina* decomposition (Philben and Benner 2013). Thus, it is likely that the greater Hyp concentrations in grazed creeks are driven by *Sesarma* grazing on *Spartina*, which releases Hyp from *Spartina* cell walls into creek-head sediments. This, coupled with the greater concentrations of γ -amino butyric acid (GABA) in grazed-creek sediment (Table S6), which typically increases during diagenesis (Cowie and Hedges 1994), further indicates that grazed creeks are sites of enhanced *Spartina* turnover (Philben and Benner 2013) and also identifies the specific compounds that are altered through *Sesarma* grazing on *Spartina*.

Our data indicate that *Sesarma* consumes *Spartina* and assimilates N-rich compounds, as seen in the loss of THAA, decline in %TN, increase in C:N, and decline in $\delta^{15}\text{N}$, between crab fore- and hind-gut samples (Figs. 4 and 5). Considering that *Sesarma* burrow densities can reach 280 m^{-2} at creek heads in this region, and that their burrowing/grazing fronts can progress across the marsh at rates exceeding several meters per year (Crotty et al. 2020), the transfer of OM from *Spartina* biomass to crab tissues likely influences OM cycling at the landscape scale and further highlights the need to incorporate invertebrate burrowing and grazing in models of salt marsh blue C storage and turnover.

Conclusions

Sesarma reticulatum directly alter marsh sedimentation and OM cycling through their grazing and burrowing activities in Georgia salt marshes. We measured multiple variables to explore how this keystone engineer influences sedimentation, hydrology, and OM cycling in salt marshes of the Southeastern USA. Radionuclides ^{7}Be and $^{210}\text{Pb}_{\text{XS}}$ indicated that grazed creeks experience greater bioturbation and longer periods of tidal inundation, which *Sesarma* require for grazing and continued creek incision (Crotty et al. 2020). We confirmed that *Spartina* is the primary food source for *Sesarma*, as determined by comparison of stable isotope values of C and N in *Sesarma* food sources and the crab's tissues. We found that, as a primary grazer of *Spartina* in this system, *Sesarma* obtains C and N, as well as N-rich amino acids from *Spartina* biomass. Additionally, fractionation processes in *Sesarma* guts resulted in a significant decline in $\delta^{15}\text{N}$ values in gut OM and excretion of ^{15}N -depleted N into grazed-creek sediments. Grazed creeks also exhibited greater %TN in their sediments, and both N measures displayed extreme values in highly grazed creek zones, suggesting that *Sesarma* also may play an important role in N cycling of grazed creeks in the region.

Sesarma grazing fronts are pervasive along the US Atlantic Seaboard and *Sesarma*-grazed creeks are incising rapidly into salt marshes of the region. These observations, along with our findings, highlight the important role that *Sesarma* plays in OM turnover, which may alter marsh biogeochemistry at the landscape scale. Given the ubiquity of Sesarmids in marshes throughout the world, there is a need to incorporate the role of fauna such as *Sesarma* in models of OM turnover in blue C habitats. Whereas other common crab species may differ in the extent of their bioturbation and herbivory, it is also important to consider their impacts in models of OM turnover in coastal ecosystems. This is particularly critical in the context of global changes such as sea level rise, and consequent ecological regime shifts such as the transition of marsh to mangrove ecosystems, which will likely lead to changes in faunal assemblages, including keystone grazers and bioturbators such as *Sesarma*. Moreover, as more marine benthos undergo range expansion in the coastal zone, largely because of global warming (e.g., (Johnson 2015; Landers et al. 2001)), we need to better understand how grazing and bioturbation will affect biogeochemical cycling in newly occupied habitats (Bianchi et al. 2021). Thus, the role of fauna in altering biogeochemical processes must be considered in forecasting the value of these habitats as blue C sinks and in evaluating the role that coastal marsh systems and their biota play in climate feedbacks.

Supplementary Information The online version contains supplementary material available at <https://doi.org/10.1007/s12237-024-01336-9>.

Acknowledgements We thank the University of Georgia Marine Institute, Georgia Coastal Ecosystems Long-Term Ecological Research Site and Sapelo Island National Estuarine Research Reserve for logistical support. We also thank Dow Van Arnam for assistance with sample collection, David Lance Malcom for assistance with sample collection and processing, and Jason Curtis for elemental and stable isotope analyses.

Funding This work was supported by a University of Florida SEED grant to Christine Angelini, Thomas S. Bianchi, William Kenney, Mark Brenner, and Alberto Canestrelli and an NSF CAREER award (#1652628) to Christine Angelini.

Declarations

Conflict of Interest The authors declare no competing interests.

Open Access This article is licensed under a Creative Commons Attribution 4.0 International License, which permits use, sharing, adaptation, distribution and reproduction in any medium or format, as long as you give appropriate credit to the original author(s) and the source, provide a link to the Creative Commons licence, and indicate if changes were made. The images or other third party material in this article are included in the article's Creative Commons licence, unless indicated otherwise in a credit line to the material. If material is not included in the article's Creative Commons licence and your intended use is not permitted by statutory regulation or exceeds the permitted use, you will need to obtain permission directly from the copyright holder. To view a copy of this licence, visit <http://creativecommons.org/licenses/by/4.0/>.

References

- Abele, L.G. 1973. Taxonomy, distribution, and ecology of genus *Sesarma* (Crustacea, Decapoda, Grapsidae) in Eastern North America, with special reference to Florida. *American Midland Naturalist* 90 (2): 375–386. <https://doi.org/10.2307/2424461>.
- Adams, T.S., and R.W. Sterner. 2000. The effect of dietary nitrogen content on trophic level N-15 enrichment. *Limnology and Oceanography* 45 (3): 601–607. <https://doi.org/10.4319/lo.2000.45.3.0601>.
- Aller, R. 1980. Quantifying the solute distributions in the bioturbated zone of marine sediments by defining an average microenvironment. *Geochimica Et Cosmochimica Acta* 44 (12): 1955–2065.
- Aller, R.C., and J.K. Cochran. 2019. The critical role of bioturbation for particle dynamics, priming potential, and organic C remineralization in marine sediments: local and basin scales. *Frontiers in Earth Science* 7. <https://doi.org/10.3389/feart.2019.00157>.
- Altieri, A.H., M.D. Bertness, T.C. Coverdale, N.C. Herrmann, and C. Angelini. 2012. A trophic cascade triggers collapse of a salt-marsh ecosystem with intensive recreational fishing. *Ecology* 93 (6): 1402–1410.
- Angelini, C., S.G. van Montfrans, M.J. Hensel, Q. He, and B.R. Silliman. 2018. The importance of an underestimated grazer under climate change: How crab density, consumer competition, and physical stress affect salt marsh resilience. *Oecologia* 187 (1): 205–217.
- Angelini, C., T. van der Heide, J.N. Griffin, J.P. Morton, M. Derkzen-Hooijberg, L.P.M. Lamers, et al. 2015. Foundation species' overlap enhances biodiversity and multifunctionality from the patch to landscape scale in southeastern United States salt

marshes. *Proceedings of the Royal Society B-Biological Sciences* 282(1811). <https://doi.org/10.1098/rspb.2015.0421>.

Angelini C, J.N Griffin, J. van de Koppel, L.P.M. Lamers, A.J.P. Smolders, M. Derkens-Hooijberg, et al. 2016. A keystone mutualism underpins resilience of a coastal ecosystem to drought. *Nature Communications* 7. <https://doi.org/10.1038/ncomms12473>.

Appleby, P. 2008. Three decades of dating recent sediments by fallout radionuclides: A review. *The Holocene* 18 (1): 83–93.

Arias-Ortiz, A., P. Masqué, J. Garcia-Orellana, O. Serrano, I. Mazarrasa, N. Marbà, et al. 2018. Reviews and syntheses: 210 Pb-derived sediment and carbon accumulation rates in vegetated coastal ecosystems—setting the record straight. *Biogeosciences* 15 (22): 6791–6818.

Aufdenkampe, A.K., J.I. Hedges, J.E. Richéy, A.V. Krusche, and C.A. Llerena. 2001. Sorptive fractionation of dissolved organic nitrogen and amino acids onto fine sediments within the Amazon Basin. *Limnology and Oceanography* 46 (8): 1921–1935. <https://doi.org/10.4319/lo.2001.46.8.1921>.

Baker, R., B. Fry, L.P. Rozas, and T.J. Minello. 2013. Hydrodynamic regulation of salt marsh contributions to aquatic food webs. *Marine Ecology Progress Series* 490: 37–52.

Baskaran, M., C.H. Coleman, and P.H. Santschi. 1993. Atmospheric depositional fluxes of 7Be and 210Pb at Galveston and College Station, Texas. *Journal of Geophysical Research: Atmospheres* 98 (D11): 20555–20571.

Bertness, M.D., C. Holdredge, and A.H. Altieri. 2009. Substrate mediates consumer control of salt marsh cordgrass on Cape Cod. *New England Ecology* 90 (8): 2108–2117. <https://doi.org/10.1890/08-1396.1>.

Bertness, M.D., C.P. Brisson, T.C. Coverdale, M.C. Bevil, S.M. Crotty, and E.R. Suglia. 2014. Experimental predator removal causes rapid salt marsh die-off. *Ecology Letters* 17 (7): 830–835. <https://doi.org/10.1111/ele.12287>.

Bianchi, T.S., and E.S. Morrison. 2018. Human activities create corridors of change in aquatic zones. *Eos* 99 (11): 13–15.

Bianchi, T.S., R.C. Aller, T.B. Atwood, C.J. Brown, L.A. Buatois, L.A. Levin, et al. 2021. What global biogeochemical consequences will marine animal–sediment interactions have during climate change? *Elementa: Science of the Anthropocene* 9 (1): 00180.

Bock, M.J., and L.M. Mayer. 1999. Digestive plasticity of the marine benthic omnivore *Nereis virens*. *Journal of Experimental Marine Biology and Ecology* 240 (1): 77–92.

Borst, A.C.W., W.C.E.P. Verberk, C. Angelini, J. Schotanus, J.-W. Wolters, M.J.A. Christianen, et al. 2018. Foundation species enhance food web complexity through non-trophic facilitation. *PLoS ONE* 13 (8): e0199152. <https://doi.org/10.1371/journal.pone.0199152>.

Costanza, R., R. de Groot, L. Braat, I. Kubiszewski, L. Fioramonti, P. Sutton, et al. 2017. Twenty years of ecosystem services: How far have we come and how far do we still need to go? *Ecosystem Services* 28: 1–16. <https://doi.org/10.1016/j.ecoser.2017.09.008>.

Cowie, G.L., and J.I. Hedges. 1994. Biochemical indicators of diagenetic alteration in natural organic-matter mixtures. *Nature* 369 (6478): 304–307. <https://doi.org/10.1038/369304a0>.

Crotty, S.M., C. Angelini, and M.D. Bertness. 2017. Multiple stressors and the potential for synergistic loss of New England salt marshes. *PLoS ONE* 12 (8): e0183058. <https://doi.org/10.1371/journal.pone.0183058>.

Crotty, S.M., C. Ortals, T.M. Pettengill, L. Shi, M. Olabarrieta, M.A. Joyce, et al. 2020. Sea-level rise and the emergence of a keystone grazer alter the geomorphic evolution and ecology of southeast US salt marshes. *Proceedings of the National Academy of Sciences of the United States of America* 117 (30): 17891–17902. <https://doi.org/10.1073/pnas.1917869117>.

Currin, C., S. Newell, and H. Paerl. 1995. The role of standing dead *Spartina alterniflora* and benthic microalgae in salt marsh food webs: Considerations based on multiple stable isotope analysis. *Marine Ecology Progress Series* 121: 99–116.

Dale, H., M. Solan, P. Lam, and M. Cunliffe. 2019. Sediment microbial assemblage structure is modified by marine polychaete gut passage. *FEMS microbiology ecology* 95 (5): fiz047.

Dauwe, B., and J.J. Middelburg. 1998. Amino acids and hexosamines as indicators of organic matter degradation state in North Sea sediments. *Limnology and Oceanography* 43 (5): 782–798. <https://doi.org/10.4319/lo.1998.43.5.0782>.

Dauwe, B., J.J. Middelburg, P.M.J. Herman, and C.H.R. Heip. 1999. Linking diagenetic alteration of amino acids and bulk organic matter reactivity. *Limnology and Oceanography* 44 (7): 1809–1814. <https://doi.org/10.4319/lo.1999.44.7.1809>.

Dinno, A. 2017. dunn.test: Dunn's test of multiple comparisons using rank sums.

Duan, S., and T.S. Bianchi. 2007. Particulate and dissolved amino acids in the lower Mississippi and Pearl Rivers (USA). *Marine Chemistry* 107 (2): 214–229. <https://doi.org/10.1016/j.marchem.2007.07.003>.

Duarte, C.M., W.C. Dennison, R.J.W. Orth, and T.J.B. Carruthers. 2008. The charisma of coastal ecosystems: Addressing the imbalance. *Estuaries and Coasts* 31 (2): 233–238. <https://doi.org/10.1007/s12237-008-9038-7>.

Farron, S., Z. Hughes, D. FitzGerald, and K. Strom. 2020. The impacts of bioturbation by common marsh crabs on sediment erodibility: A laboratory flume investigation. *Estuarine, Coastal and Shelf Science* 238.

Friesen, S.D., C. Dunn, and C. Freeman. 2018. Decomposition as a regulator of carbon accretion in mangroves: A review. *Ecological Engineering* 114: 173–178. <https://doi.org/10.1016/j.ecoleng.2017.06.069>.

Ganju, N.K., Z. Defne, M.L. Kirwan, S. Fagherazzi, A. D'Alpaos, and L. Carniello. 2017. Spatially integrative metrics reveal hidden vulnerability of microtidal salt marshes. *Nature Communications* 8 (1): 1–7.

Gannes, L.Z., C.M. del Rio, and P. Koch. 1998. Natural abundance variations in stable isotopes and their potential uses in animal physiological ecology. *Comparative Biochemistry and Physiology a-Molecular and Integrative Physiology* 119 (3): 725–737. [https://doi.org/10.1016/s1095-6433\(98\)01016-2](https://doi.org/10.1016/s1095-6433(98)01016-2).

Gilbert, F., R.C. Aller, and S. Hulth. 2003. The influence of macrofaunal burrow spacing and diffusive scaling on sedimentary nitrification and denitrification: An experimental simulation and model approach. *Journal of Marine Research* 61 (1): 101–125. <https://doi.org/10.1357/002224003321586426>.

Guimond, J.A., A.L. Seyfferth, K.B. Moffett, H.A. Michael. 2020. A physical-biogeochemical mechanism for negative feedback between marsh crabs and carbon storage. *Environmental Research Letters* 15(3). <https://doi.org/10.1088/1748-9326/ab60e2>.

Harris, D., W.R. Horwath, and C. van Kessel. 2001. Acid fumigation of soils to remove carbonates prior to total organic carbon or carbon-13 isotopic analysis. *Soil Science Society of America Journal* 65 (6): 1853–1856. <https://doi.org/10.2136/sssaj2001.1853>.

He, Q., H. Li, C. Xu, Q. Sun, M.D. Bertness, C. Fang, et al. 2020. Consumer regulation of the carbon cycle in coastal wetland ecosystems. *Philosophical Transactions of the Royal Society B-Biological Sciences* 375(1814). <https://doi.org/10.1098/rstb.2019.0451>.

Henrichs, S.M., and J.W. Farrington. 1987. Early diagenesis of amino acids and organic matter in 2 coastal marine sediments. *Geochimica Et Cosmochimica Acta* 51 (1): 1–15. [https://doi.org/10.1016/0016-7037\(87\)90002-0](https://doi.org/10.1016/0016-7037(87)90002-0).

Herbon, C.M., and I. Nordhaus. 2013. Experimental determination of stable carbon and nitrogen isotope fractionation between mangrove leaves and crabs. *Marine Ecology Progress Series* 490: 91–105. <https://doi.org/10.3354/meps10421>.

Hinson, A.L., R.A. Feagin, M. Eriksson, R.G. Najjar, M. Herrmann, T.S. Bianchi, et al. 2017. The spatial distribution of soil organic carbon in tidal wetland soils of the continental United States. *Global Change Biology* 23 (12): 5468–5480. <https://doi.org/10.1111/gcb.13811>.

Holdredge, C., M.D. Bertness, and A.H. Altieri. 2009. Role of crab herbivory in die-off of New England salt marshes. *Conservation Biology* 23 (3): 672–679. <https://doi.org/10.1111/j.1523-1739.2008.01137.x>.

Hopkinson, C.S., W.-J. Cai, and X. Hu. 2012. Carbon sequestration in wetland dominated coastal systems - a global sink of rapidly diminishing magnitude. *Current Opinion in Environmental Sustainability* 4 (2): 186–194. <https://doi.org/10.1016/j.cosust.2012.03.005>.

Hughes, Z.J., D.M. FitzGerald, C.A. Wilson, S.C. Pennings, K. Więski, A. Mahadevan. 2009. Rapid headward erosion of marsh creeks in response to relative sea level rise. *Geophysical Research Letters* 36(3).

Hutchings, J.A., M.R. Shields, T.S. Bianchi, and E.A.G. Schuur. 2018. A rapid and precise method for the analysis of underivatized amino acids in natural samples using volatile-ion-pairing reverse-phase liquid chromatography-electrospray ionization tandem mass spectrometry. *Organic Geochemistry* 115: 46–56. <https://doi.org/10.1016/j.orggeochem.2017.10.007>.

Ingalls, A.E., C. Lee, S.G. Wakeham, and J.I. Hedges. 2003. The role of biominerals in the sinking flux and preservation of amino acids in the Southern Ocean along 170 degrees W. *Deep-Sea Research Part II-Topical Studies in Oceanography* 50 (3–4): 713–738. [https://doi.org/10.1016/s0967-0645\(02\)00592-1](https://doi.org/10.1016/s0967-0645(02)00592-1).

Isenburg, M. 2020 LAStools—efficient LiDAR processing software. Available online: lastools.org (version 200813, academic)

Jardine, T.D., R.A. Curry, K.S. Heard, and R.A. Cunjak. 2005. High fidelity: Isotopic relationship between stream invertebrates and their gut contents. *Journal of the North American Benthological Society* 24 (2): 290–299. <https://doi.org/10.1899/04-092.1>.

Johnson, D.S. 2015. The savory swimmer swims north: A northern range extension of the blue crab *Callinectes sapidus*? *Journal of Crustacean Biology* 35 (1): 105–110.

Kearney, W.S., and S. Fagherazzi. 2016. Salt marsh vegetation promotes efficient tidal channel networks. *Nature Communications* 7 (1): 12287.

Krishnaswamy, S., D. Lal, J. Martin, and M. Meybeck. 1971. Geochronology of lake sediments. *Earth and Planetary Science Letters* 11 (1–5): 407–414.

Kristensen, E. 2000. Organic matter diagenesis at the oxic/anoxic interface in coastal marine sediments, with emphasis on the role of burrowing animals. *Hydrobiologia* 426 (1–3): 1–24. <https://doi.org/10.1023/a:1003980226194>.

Kristensen, E. 2008. Mangrove crabs as ecosystem engineers; with emphasis on sediment processes. *Journal of Sea Research* 59 (1–2): 30–43. <https://doi.org/10.1016/j.seares.2007.05.004>.

Kristensen, E., and J.E. Kostka. 2005. Macrofaunal burrows and irrigation in marine sediment: Microbiological and biogeochemical interactions. *Interactions between Macro- and Microorganisms in Marine Sediments* 60: 125–157.

Kristensen, D.K., E. Kristensen, and P. Mangion. 2010. Food partitioning of leaf-eating mangrove crabs (Sesarmaeinae): Experimental and stable isotope (C-13 and N-15) evidence. *Estuarine Coastal and Shelf Science* 87 (4): 583–590. <https://doi.org/10.1016/j.ecss.2010.02.016>.

Landers, D.F., Jr., M. Keser, and S.B. Saila. 2001. Changes in female lobster (*Homarus americanus*) size at maturity and implications for the lobster resource in Long Island Sound. *Connecticut. Marine and Freshwater Research* 52 (8): 1283–1290.

Langston, A.K., C.R. Alexander, M. Alber, and M.L. Kirwan. 2021. Beyond 2100: Elevation capital disguises salt marsh vulnerability to sea-level rise in Georgia, USA. *Estuarine, Coastal and Shelf Science* 249.

Laverock, B., J.A. Gilbert, K. Tait, A.M. Osborn, and S. Widdicombe. 2011. Bioturbation: Impact on the marine nitrogen cycle. *Biochemical Society Transactions* 39: 315–320. <https://doi.org/10.1042/bst0390315>.

Laverock, B., V. Kitidis, K. Tait, J.A. Gilbert, A.M. Osborn, S. Widdicombe. 2013. Bioturbation determines the response of benthic ammonia-oxidizing microorganisms to ocean acidification. *Philosophical Transactions of the Royal Society B-Biological Sciences* 368(1627). <https://doi.org/10.1098/rstb.2012.0441>.

Lee, C., S.G. Wakeham, and J.I. Hedges. 2000. Composition and flux of particulate amino acids and chloropigments in equatorial Pacific seawater and sediments. *Deep-Sea Research Part I-Oceanographic Research Papers* 47 (8): 1535–1568. [https://doi.org/10.1016/s0967-0637\(99\)00116-8](https://doi.org/10.1016/s0967-0637(99)00116-8).

Linton, S.M. 2020. Review: the structure and function of cellulase (endo-beta-1,4-glucanase) and hemicellulase (beta-1,3-glucanase and endo-beta-1,4-mannase) enzymes in invertebrates that consume materials ranging from microbes, algae to leaf litter. *Comparative Biochemistry and Physiology B-Biochemistry & Molecular Biology* 240. <https://doi.org/10.1016/j.cbpb.2019.110354>.

Macreadie, P.I., A. Anton, J.A. Raven, N. Beaumont, R.M. Connolly, D.A. Friess, et al. 2019. The future of Blue Carbon science (vol 10, 3998, 2019). *Nature Communications* 10: 1. <https://doi.org/10.1038/s41467-019-13126-0>.

Martínez-Soto, K.S., and D.S. Johnson. 2023. A fiddler crab reduces plant growth in its expanded range. *Ecology* e4203.

Mayer, L.M. 1989. Extracellular proteolytic enzyme activity in sediments of an intertidal mudflat. *Limnology and Oceanography* 34 (6): 973–981.

Mayer, L.M., L.S. Linda, T. Sawyer, C.J. Plante, P.A. Jumars, and R.L. Sel. 1995. Bioavailable amino acids in sediments: A biomimetic, kinetics based approach. *Limnology and Oceanography* 40 (3): 511–520.

McCrath, B.J., L.R. Gardner, D.S. Wethey, and W.S. Moore. 2003. The effect of fiddler crab burrowing on sediment mixing and radionuclide profiles along a topographic gradient in a southeastern salt marsh. *Journal of Marine Research* 61 (3): 359–390.

McCutchan, J.H., W.M. Lewis, C. Kendall, and C.C. McGrath. 2003. Variation in trophic shift for stable isotope ratios of carbon, nitrogen, and sulfur. *Oikos* 102 (2): 378–390. <https://doi.org/10.1034/j.1600-0706.2003.12098.x>.

McLeod, E., G.L. Chmura, S. Bouillon, R. Salm, M. Bjork, C.M. Duarte, et al. 2011. A blueprint for blue carbon: Toward an improved understanding of the role of vegetated coastal habitats in sequestering CO2. *Frontiers in Ecology and the Environment* 9 (10): 552–560. <https://doi.org/10.1890/110004>.

Michaud, E., G. Desrosiers, R.C. Aller, F. Mermilliod-Blondin, B. Sundby, and G. Stora. 2009. Spatial interactions in the *Macoma balthica* community control biogeochemical fluxes at the sediment-water interface and microbial abundances. *Journal of Marine Research* 67 (1): 43–70. <https://doi.org/10.1357/002224009788597926>.

Micheli, F. 1993. Feeding ecology of mangrove crabs in North Eastern Australia: Mangrove litter consumption by *Sesarma messa* and *Sesarma smithii*. *Journal of Experimental Marine Biology and Ecology* 171 (2): 165–186.

Middelburg, J.J. 2014. Stable isotopes dissect aquatic food webs from the top to the bottom. *Biogeosciences* 11 (8): 2357–2371. <https://doi.org/10.5194/bg-11-2357-2014>.

Middelburg, J.J. 2018. Reviews and syntheses: To the bottom of carbon processing at the seafloor. *Biogeosciences* 15 (2): 413–427. <https://doi.org/10.5194/bg-15-413-2018>.

Morrison, E.S., T.S. Bianchi, W.F. Kenney, M. Brenner, K.D. Prince, C. Ortals, et al. 2022. Sediment, crab, and vegetation data from Sapelo Island, Georgia: 2017 - 2019 ver 1. <https://doi.org/10.6073/pasta/9f4f43b8bf95c28896fcb1d8ef5f020b>: Environmental Data Initiative

Morrison, E.S., M.R. Shields, T.S. Bianchi, Y. Liu, S. Newman, N. Tolic, et al. 2020. Multiple biomarkers highlight the importance of water column processes in treatment wetland organic matter cycling. *Water Research* 168. <https://doi.org/10.1016/j.watres.2019.115153>.

Ortals, C., O. Cordero, A. Valle-Levinson, and C. Angelini. 2021. Flows, transport, and effective drag in intertidal salt marsh

creeks. *Journal of Geophysical Research: Oceans* 126 (11): e2021JC017357.

Perger, D.A.S., I.P. Dwyer, R.C. Aller, N. Volkenborn, C. Heilbrun, L.M. Wehrmann. 2023. Seasonal iron fluxes and iron cycling in sandy bioirrigated sediments. *Frontiers in Marine Science*

Philben, M., and R. Benner. 2013. Reactivity of hydroxyproline-rich glycoproteins and their potential as biochemical tracers of plant-derived nitrogen. *Organic Geochemistry* 57: 11–22. <https://doi.org/10.1016/j.orggeochem.2013.01.003>.

Philben, M., S.E. Ziegler, K.A. Edwards, R. Kahler III., and R. Benner. 2016. Soil organic nitrogen cycling increases with temperature and precipitation along a boreal forest latitudinal transect. *Biogeochemistry* 127 (2–3): 397–410. <https://doi.org/10.1007/s10533-016-0187-7>.

Prince, K.D., S.M. Crotty, A. Cetta, J.J. Delfino, T.M. Palmer, N.D. Denslow, et al. 2021. Mussels drive polychlorinated biphenyl (PCB) biomagnification in a coastal food web. *Scientific Reports* 11 (1): 1–11.

Robertson, A. 1986. Leaf-burying crabs: their influence on energy flow and export from mixed mangrove forests (*Rhizophora* spp.) in northeastern Australia. *Journal of experimental marine biology and ecology* 102 (2–3): 237–48.

Rochlin, I., and J.T. Morris. 2017. Regulation of salt marsh mosquito populations by the 18.6-yr lunar-nodal cycle. *Ecology* 98 (8): 2059–68.

Schelske, C.L., A. Peplow, M. Brenner, and C.N. Spencer. 1994. Low-background gamma counting: Applications for 210 Pb dating of sediments. *Journal of Paleolimnology* 10 (2): 115–128.

Self, R.F., P.A. Jumars, and L.M. Mayer. 1995. In vitro amino acid and glucose uptake rates across the gut wall of a surface deposit feeder. *Journal of Experimental Marine Biology and Ecology* 192 (2): 289–318.

Silliman, B.R., and A. Bortolus. 2003. Underestimation of *Spartina* productivity in western Atlantic marshes: Marsh invertebrates eat more than just detritus. *Oikos* 101 (3): 549–554.

Slim, F., M. Hemminga, C. Ochieng, N. Jannink, E.C. De La Moriniere, and G. Van der Velde. 1997. Leaf litter removal by the snail *Terebralia palustris* (*Linnaeus*) and sesarmid crabs in an East African mangrove forest (Gazi Bay, Kenya). *Journal of Experimental Marine Biology and Ecology* 215 (1): 35–48.

Smith, J.M., and R.W. Frey. 1985. Biodeposition by the ribbed mussel *Geukensia demissa* in a salt marsh, Sapelo Island, Georgia. *Journal of Sedimentary Petrology* 55 (6): 817–828.

Smith, S.M., and M.C. Tyrrell. 2012. Effects of mud fiddler crabs (*Uca pugnax*) on the recruitment of halophyte seedlings in salt marsh dieback areas of Cape Cod (Massachusetts, USA). *Ecological Research* 27 (1): 233–237.

Snelgrove, P.V.R., K. Soetaert, M. Solan, S. Thrush, C.-L. Wei, R. Danovaro, et al. 2018. Global carbon cycling on a heterogeneous seafloor. *Trends in Ecology & Evolution* 33 (2): 96–105. <https://doi.org/10.1016/j.tree.2017.11.004>.

Stevenson, F.J. 1994. Humus chemistry: genesis, composition, reactions. *Humus chemistry: genesis, composition, reactions*. (Ed. 2):xiii + 496 pp.-xiii + pp.

Temmink, R.J.M., L.P.M. Lamers, C. Angelini, T.J. Bouma, C. Fritz, J. van de Koppel, et al. 2022. Recovering wetland biogeomorphic feedbacks to restore the world's biotic carbon hotspots. *Science* 376 (6593): eabn1479. <https://doi.org/10.1126/science.abn1479>.

Vaughn, D.R., T.S. Bianchi, M.R. Shields, W.F. Kenney, T.Z. Osborne. 2020 Increased organic carbon burial in northern Florida mangrove-salt marsh transition zones. *Global Biogeochemical Cycles* 34(5). <https://doi.org/10.1029/2019gb006334>.

Vu, H.D., and S.C. Pennings. 2021. Directional movement of consumer fronts associated with creek heads in salt marshes. *Ecology* 102 (9): e03447.

Vu, H.D., K. Wieski, and S.C. Pennings. 2017. Ecosystem engineers drive creek formation in salt marshes. *Ecology* 98 (1): 162–174. <https://doi.org/10.1002/ecy.1628>.

Wakeham, S.G., and C. Lee. 2019. Limits of our knowledge, part 2: Selected frontiers in marine organic biogeochemistry. *Marine Chemistry* 212: 16–46. <https://doi.org/10.1016/j.marchem.2019.02.005>.

Ward, N.D., J.P. Megonigal, B. Bond-Lamberty, V.L. Bailey, D. Butman, E.A. Canuel, et al. 2020. Representing the function and sensitivity of coastal interfaces in Earth system models. *Nature Communications* 11(1). <https://doi.org/10.1038/s41467-020-16236-2>.

Wilson, C., Z. Hughes, and D. FitzGerald. 2012. The effects of crab bioturbation on Mid-Atlantic saltmarsh tidal creek extension: Geotechnical and geochemical changes. *Estuarine, Coastal and Shelf Science* 106: 33–44.

Windham-Myers, L. S. Crooks, T. Troxler. 2018. *A blue carbon primer: the state of coastal wetland carbon science, practice and policy*. CRC Press.

Woulds, C., J.J. Middelburg, and G.L. Cowie. 2012. Alteration of organic matter during infaunal polychaete gut passage and links to sediment organic geochemistry. Part I: Amino acids. *Geochimica Et Cosmochimica Acta* 77: 396–414. <https://doi.org/10.1016/j.gca.2011.10.042>.

Wu, F., S.C. Pennings, C. Ortals, J. Ruiz, W.R. Farrell, S.M. McNichol, et al. 2021. Disturbance is complicated: Headward-eroding salt-marsh creeks produce multiple responses and recovery trajectories. *Limnology and Oceanography*

Xiao, K., A.M. Wilson, H. Li, I.R. Santos, J. Tamborski, E. Smith, et al. 2021. LargeCO₂ release and tidal flushing in salt marsh crab burrows reduce the potential for blue carbon sequestration. *Limnology and Oceanography* 66 (1): 14–29. <https://doi.org/10.1002/lnco.11582>.

Zhang, X., L. Cui, M. Nie, J. Shao, S. Wei, X. Kang, et al. 2019. Macrophytes and crabs affect nitrogen transformations in salt marshes of the Yangtze River Estuary. *Estuarine Coastal and Shelf Science* 225. <https://doi.org/10.1016/j.ecss.2019.106242>.

Authors and Affiliations

Elise S. Morrison¹  · Thomas S. Bianchi² · William F. Kenney³ · Mark Brenner^{2,3} · Kimberly Prince^{1,4} ·
Sydney Williams¹ · Collin Ortals¹ · Orlando Cordero¹ · Sinéad M. Crotty^{1,5} · Christine Angelini¹

 Elise S. Morrison
emorrison@ufl.edu

¹ Engineering School of Sustainable Infrastructure and Environment, University of Florida, Gainesville, FL 32611, USA

² Department of Geological Sciences, University of Florida, Gainesville, FL 32611, USA

³ Land Use and Environmental Change Institute, University of Florida, Gainesville, FL 32611, USA

⁴ Department of Biological Sciences, George Washington University, Washington, DC 20052, USA

⁵ Carbon Containment Lab, Yale School of the Environment, New Haven, CT 06511, USA